SAND2011-8005C

Two dimensional laser-collision induced fluorescence measurements in low pressure plasmas

15th International Symposium on

Laser-Aided Plasma Diagnostics (LAPD)

Jeju, Korea, October 9'th - 13'th 2011

Edward V. Barnat

Sandia National Laboratories

Albuquerque, N.M., United States of America

This work was supported by the Department of Energy Office of Fusion Energy Science
Contract DE-SC0001939

Sandia National Laboratories is a multi-program laboratory managed and operated by Sandia Corporation, a wholly owned subsidiary of Lockheed Martin Corporation, for the U.S. Department of Energy's National Nuclear Security Administration under contract DE-AC04-94AL85000.

LOCKHEED MARTIN

Sandia National Laboratories

Laser-collision induced fluorescence provides measure of electron density and "temperature"

- **Motivation: What is the density? What is the temperature? Where and When?**
  - More traditional probe techniques may couple and perturb
  - Optically passive techniques are line-of-sight limited
  - Optically active-techniques such as Thomson scattering pose their own set of challenges

- **In this presentation**
  - Laser-collision induced fluorescence (LCIF) primer
    - Collisional-radiative model used to predict LCIF
    - Applied to triplet manifold of Helium
  - Implement and benchmark technique
    - Experimental setup
    - Time evolution of LCIF and time integrated LCIF
  - Applications of LCIF:
    - Ion sheaths, transient double layers, positive columns
  - Future directions and concluding comments
    - Extension of helium
    - Investigate argon

Sandia National Laboratories

Part I: LCIF concepts and key trends

- **Overview**
  - LCIF concepts
  - Collisional-radiative model for helium
  - Key scaling trends

LCIF Concept

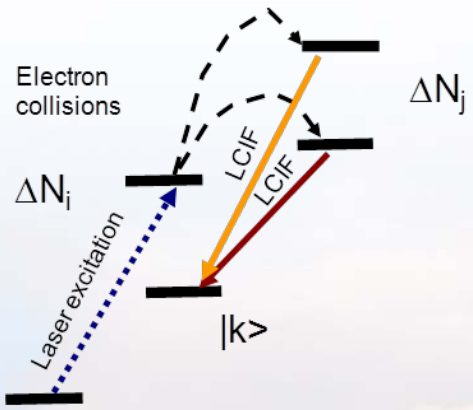

CR Model

$$\frac{dN_j}{dt} = \left[\sum_{i \neq j} K^e_{ij} N_i - \sum_{i \neq j} K^e_{ji} N_j\right] n_e + ...$$

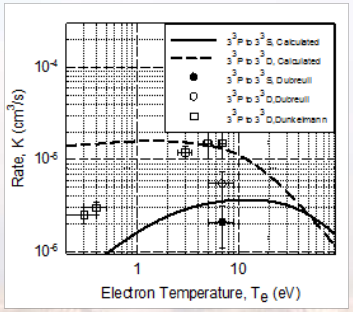

Key scaling trends

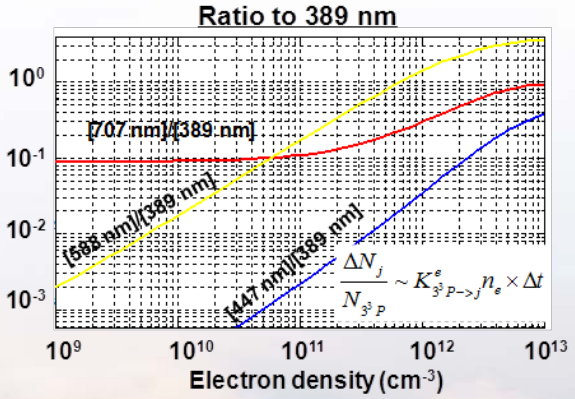

Sandia National Laboratories

LCIF is based on redistribution of excited state by plasma electrons

- **Laser excitation causes populates an intermediate state**
  - Relaxation processes deplete excited state
- **Portion of excited state population gets redistributed into "uphill" states**
  - Driven by interaction with energetic plasma electrons

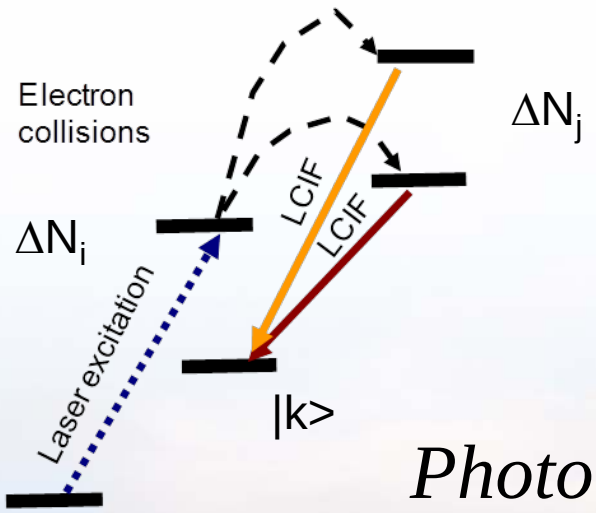

Electron- coupled interaction

$$\Delta N_j \sim K_{ij}^{e} n_e \times \Delta N_i \times \Delta t$$

Change in upper state due to excited state

$$Photons\ emitted \sim A_{jk} \times \Delta N_j \times \Delta t$$

Detected light

LCIF looks for changes in emission of neighboring states after laser excitation

Redistribution after laser excitation is complex

- **A "good" model is required to predict transfer between levels**
  - Employ a collisional-radiative model (CRM) to predict redistribution

"Electron mixing" ***"Photon mixing"*** ***"Neutral mixing"***

$$\frac{dN_j}{dt} = \left[\sum_{i\neq j} K^e_{ij} N_i - \sum_{i\neq j} K^e_{ji} N_j\right] n_e + \left[\sum_{i>j} A_{ij} N_i - \sum_{i<j} A^j_{ji} N_j\right] + \sum_k \left[\sum_{i\neq j} K^a_{ikj} N_i - \sum_{i\neq j} K^a_{jki} N_j\right] N_k$$

- **Electron density and electron temperature appear in first term**
  - Temperature dependence introduced via K^e_{ij}

Electron-temperature dependent rates

$$K^e_{ij} = \left\langle \sigma_{ij}(E) v_e \right\rangle$$

Distribution function used for describing electron velocities

$$f(v) \sim e^{(1/2 mv)^x / kT}$$

Approach is applicable to various atomic and molecular systems of interest

Helium atom serves as target species for LCIF measurements

- **Employ Helium to start with - considering argon**
  - "Simple system" with "better known" rates
- **Utilize functionalized form of cross-sections compiled by Ralchenko[1]**
  - Integrate to get rates, compare to measured rates [2,3]

Key transitions

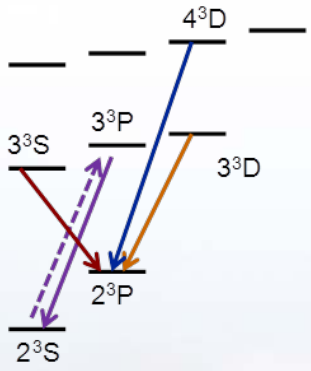

Computed and measured excitation rates in Helium

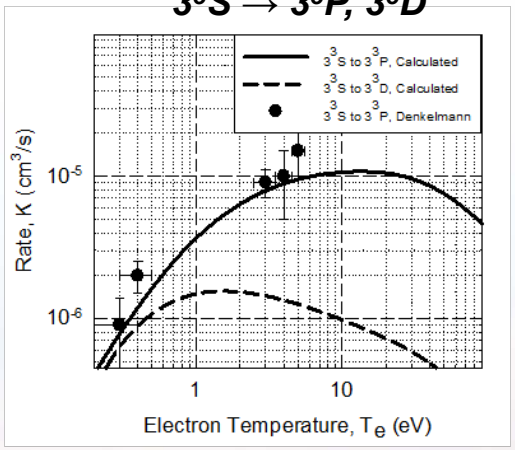

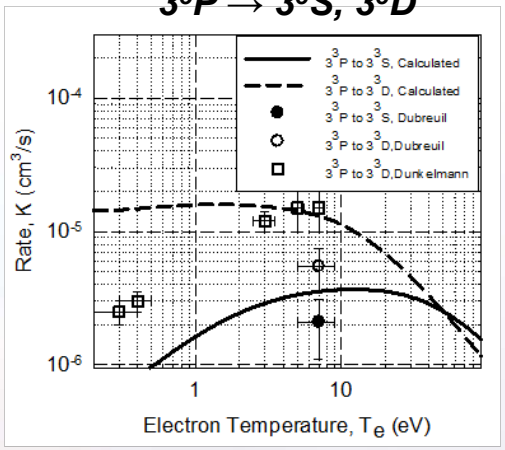

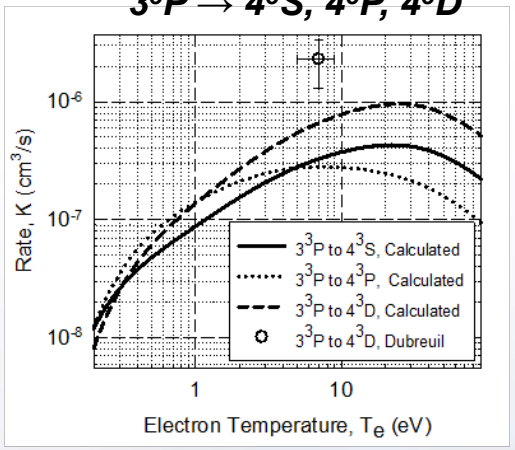

1: Yu. Ralchenko, R. K. Janev, T. Kato, D. V. Fursa, I. Bray, F. J. De Heer, Atomic Data and Nuclear Data Tables **94**, 603 (2008)
2: R. Denkelmann, S.Maurmann, T. Lokajczyk, P. Drepper, and H. –J. Kunze, J. Phys. B: At. Mol. Opt. Phys. **32**, 4635 (1999).
R. Denkelmann, S. Freund and S. Maurmann, Contrib. Plasma Phys. **40**, 91 (2000).
3: B. Dubreuil and P. Prigent, J. Phys. B: At. Mol. Opt. Phys. **18**, 4597 (1985).

Accuracy of n_e, T_e depend on knowledge of $K_{ij}(kT_e)$

Sandia National Laboratories

CRM predicts evolution of various helium states after laser excitation

- **Temporal evolution serves as a partial "fingerprint" of electron interaction**
  - Analyze shape of decay above $n_e \sim 10^{11}$ electrons/cm^3
  - Below $n_e \sim 10^{11}$ absolute intensities are needed

$$K_{ij}^{e} n_e \sim A_{ij} \quad \Rightarrow \quad 10^{-5} \times 10^{11} \sim 10^{7}$$

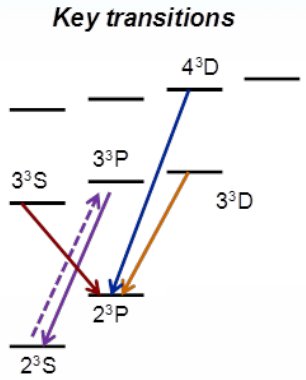

Computed temporal evolution

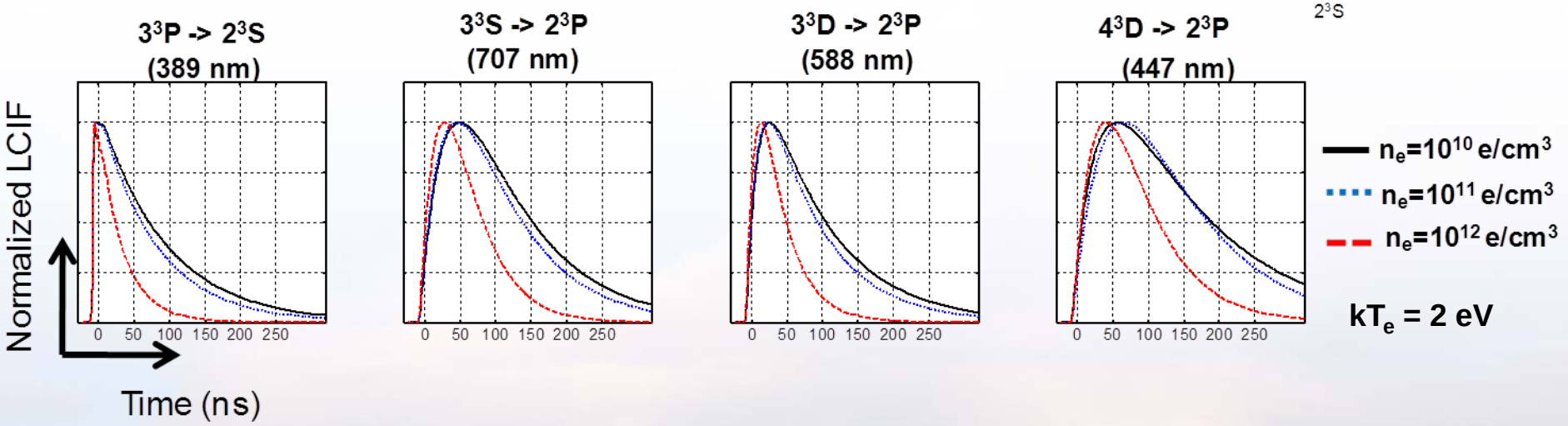

Need at least two time-resolved profiles to uniquely obtain n_e, kT_e

Time integrated intensity trends are utilized instead of time resolved LCIF

- **Examine ratios of time integrated LCIF**
  - Eliminates need for absolute calibrations
  - Still need relative efficiencies of imaging system
- **Capitalize on "kT_e independent" coupling of 3^3P to 3^3D**
  - Ratio of 588 nm to 389 nm yields n_e
  - Density + Ratio of 447nm to 588 nm yields kT_e

Window of integration

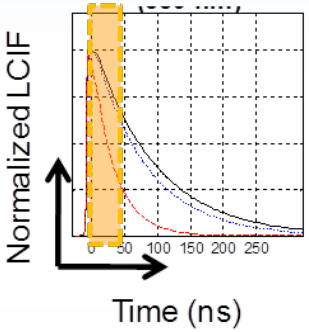

Ratio to 389 nm

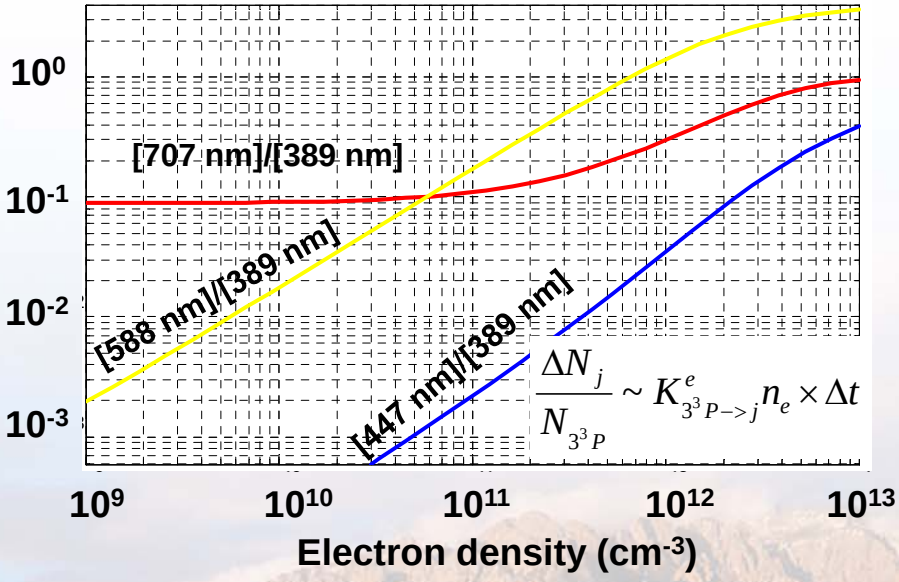

Ratio [447 nm]/[588 nm]

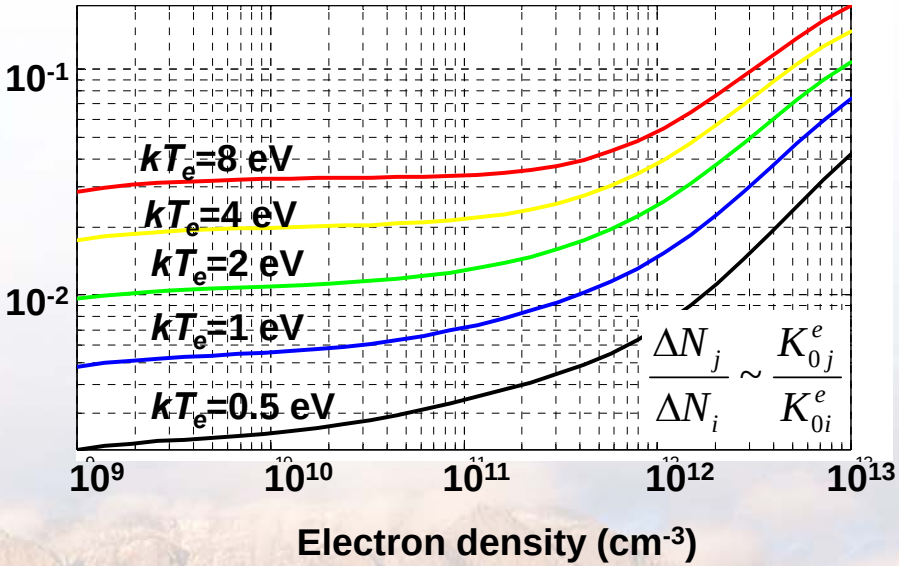

Only need to make three measurements to obtain n_e, kT_e

Sandia National Laboratories

Small energy gap leads to "kT$_e$ independent" coupling of 3^{3}P to 3^{3}D

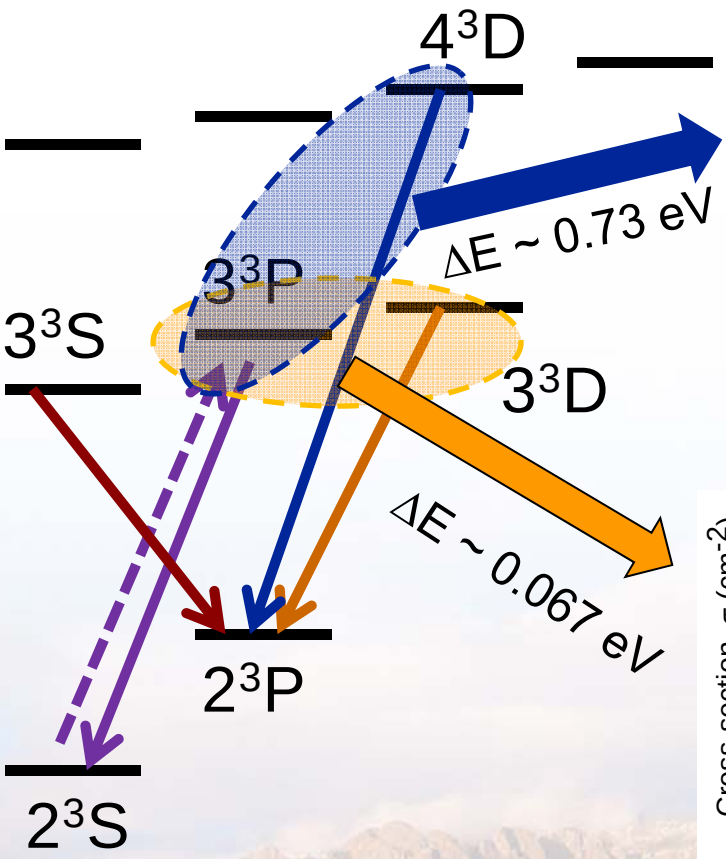

3³P → 4³D

Cross-sections

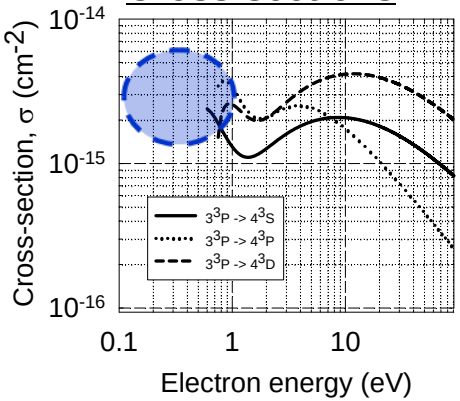

Rates

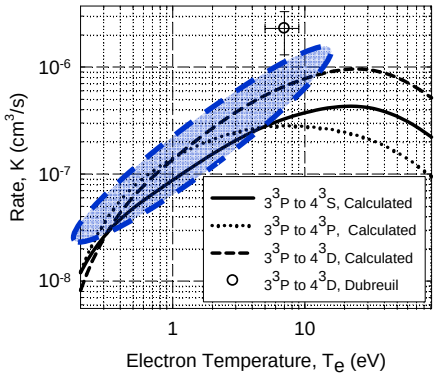

3³P → 3³D

Cross-sections

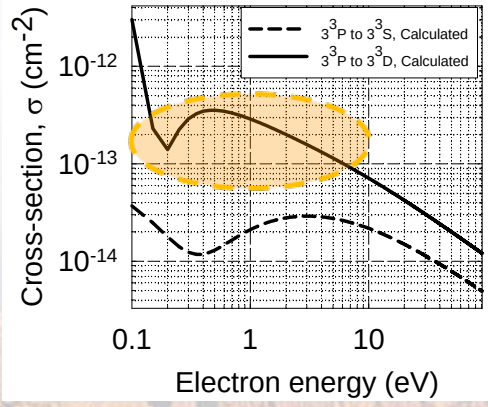

Rates

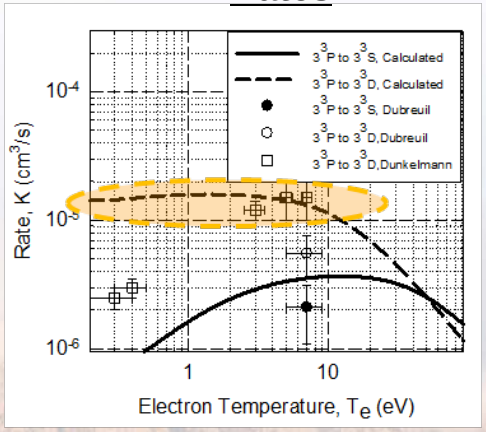

Considerable fraction of the electrons are capable of driving the interaction

Sandia National Laboratories

Yu. Ralchenko, R. K. Janev, T. Kato, D. V. Fursa, I. Bray, F. J. De Heer, Atomic Data and Nuclear Data Tables **94**, 603 (2008)

Part II: LCIF implementation and benchmark

- **Implement and benchmark technique**
  - Experimental considerations
  - Benchmarking LCIF - compare observations with anticipated trends

Experimental setup

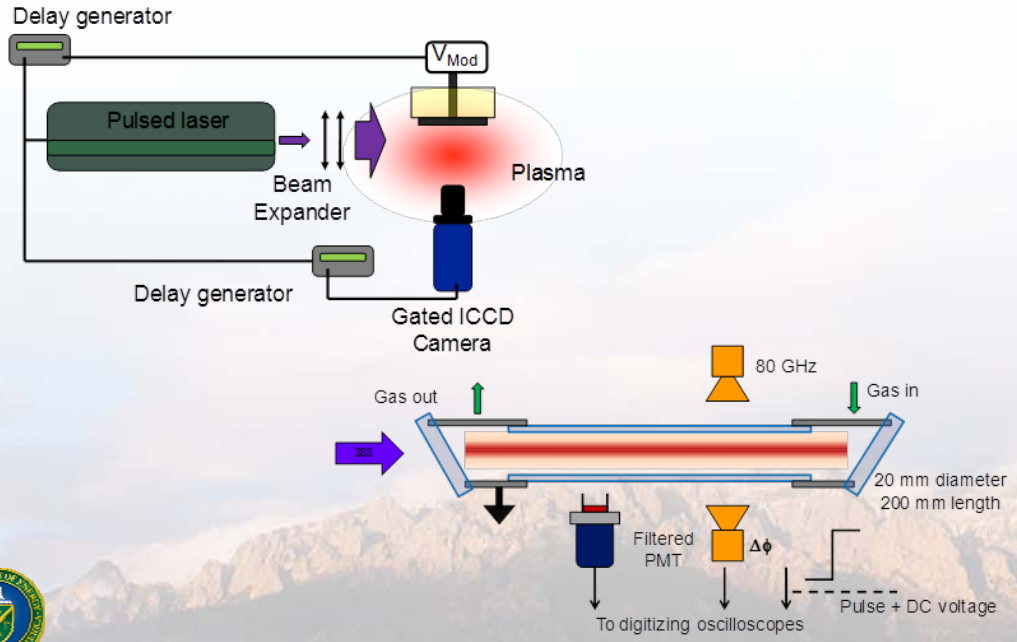

Benchmark LCIF

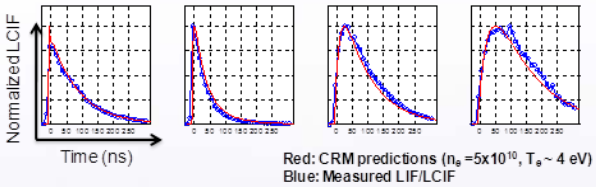

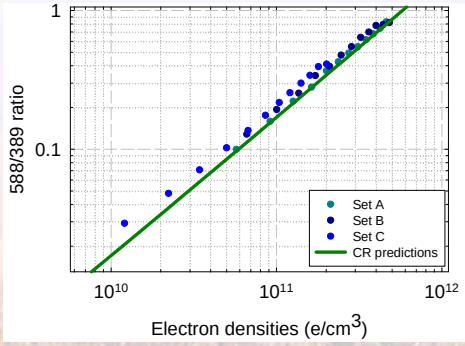

Experimental implementation of the LCIF is realized

- **Nanosecond pulsed laser used for excitation**
  - < 10 ns FWHM, < 0.1 cm^{-1} line width
- **Timing of experiment controlled by delay generators**
  - Move experiment and imaging with respect to firing of the laser
- **Image LCIF with gated-intensified CCD**
  - Narrow (~ 1 nm FWHM) interference filters centered on lines of interest
- **Take two images per transition considered**
  - Total emission and plasma induced emission (PIE) - subtract the two

Optical setup

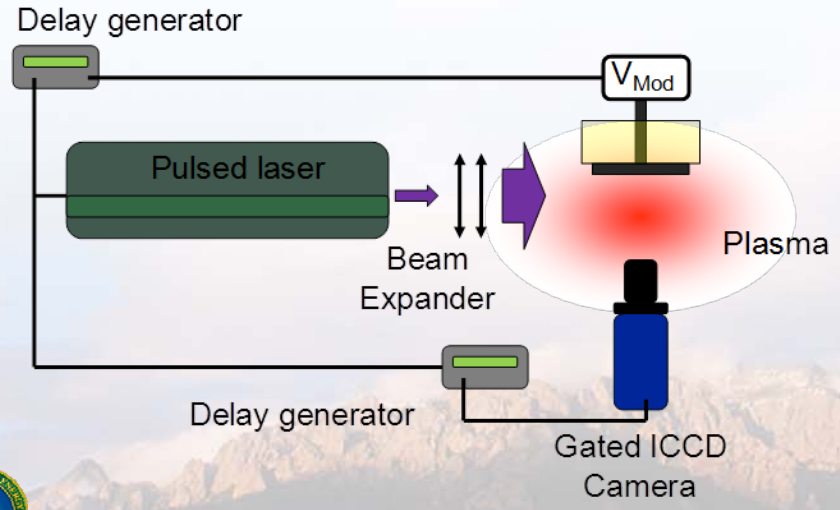

Timing sequence

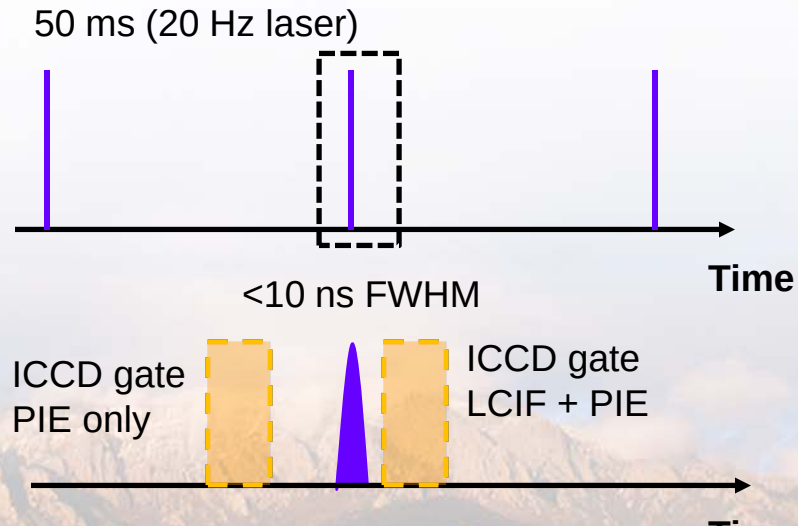

Need to make six (3 x 2) measurements to obtain n_e, kT_e

Sandia National Laboratories

Pulsed positive column is utilized to benchmark LCIF technique

- **Pulse discharge currents generate broad density range**
  - ~ 10 Microseconds, 80 GHz interferometer
- **Compute drift velocities and extract electron temperatures**
  - Use published drift parameters

Positive column

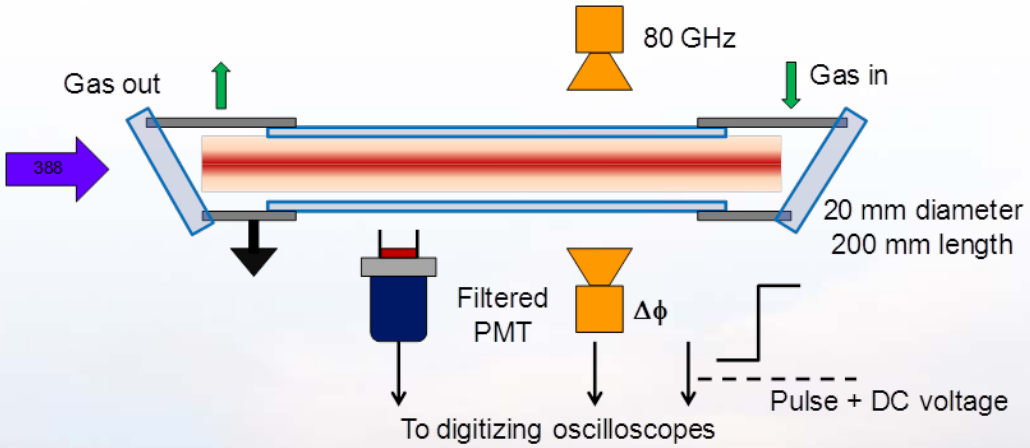

Helium drift parameters

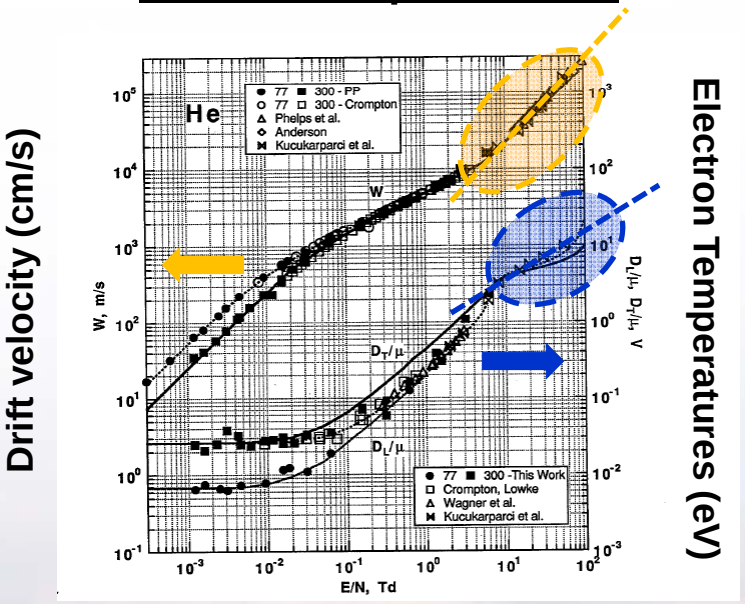

Drift velocity (cm/s)

Electron Temperatures (eV)

E/N (Td)

Positive column is a good vehicle to benchmark LCIF technique

Sandia National Laboratories

J. L. Pack, R. E. Voshall, A.V. Phelps and L. E. Kline, J. Appl. Phys. V71, p5363 (1992)

First steps: Verify time resolved LCIF to test CRM

- **First sets of measurements presented some surprises**
  - Strong radiative coupling between 3^3P and 3^3S states
- **Proper accounting produced observed trends**
  - Measured data and predicted behavior are consistent

Key transitions

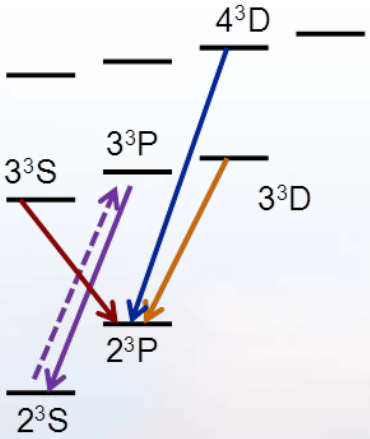

Representative results

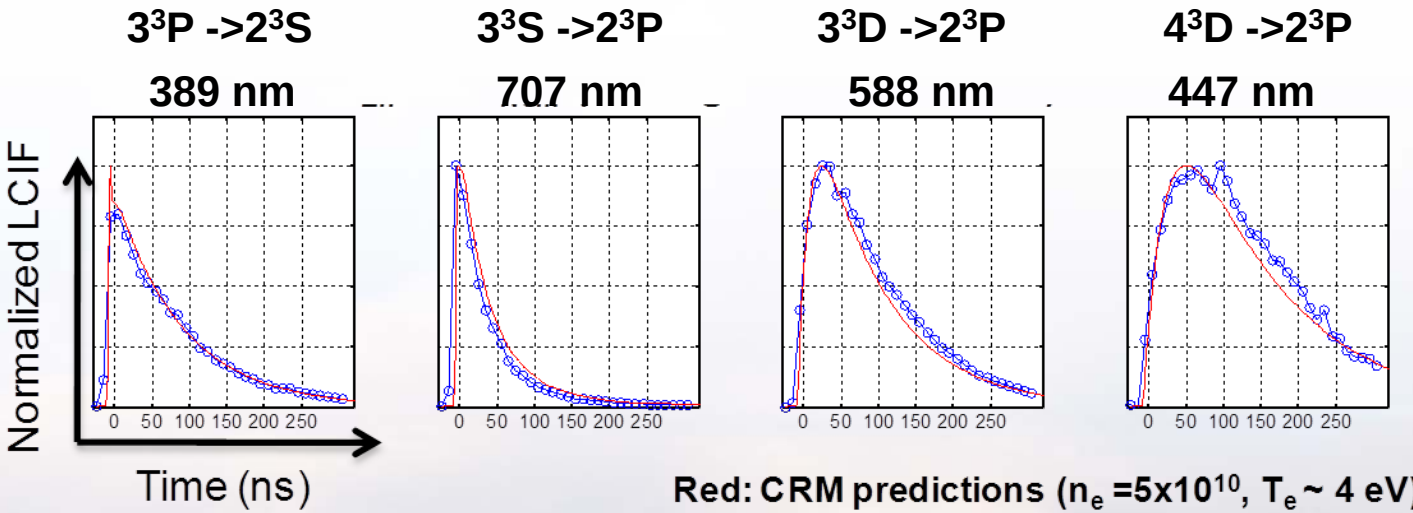

Red: CRM predictions (n_e =5x10^{10}, T_e ~ 4 eV)
Blue: Measured LIF/LCIF

Good first demonstration of LCIF technique

[588]/[389] ratio exhibits linearity over nearly two orders of magnitude

- **Better yet, measured ratios agree reasonably well with computed ratios**
  - Slightly higher, and some deviation at low density
- **Examined trends at different times during the current pulse**
  - Anticipate different temperatures as column is established

Waveforms during excitation

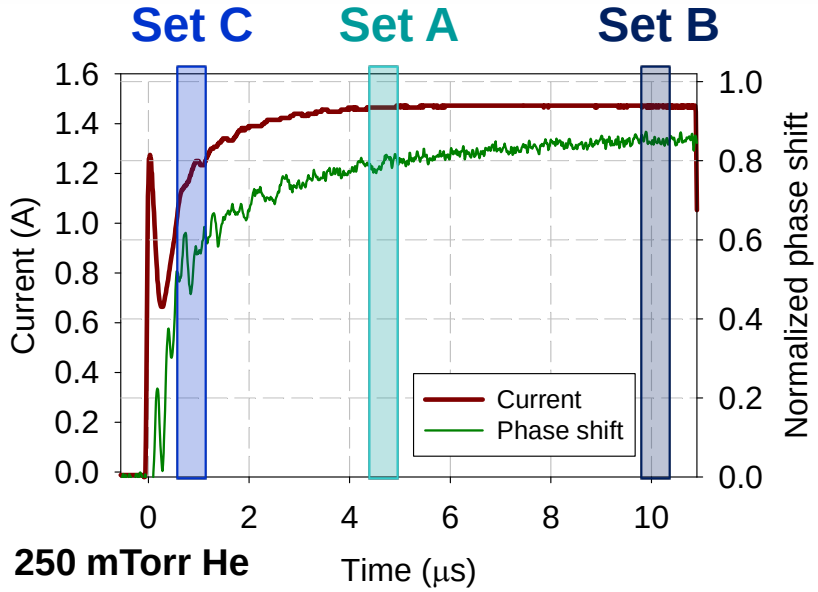

Density dependent ratio trends

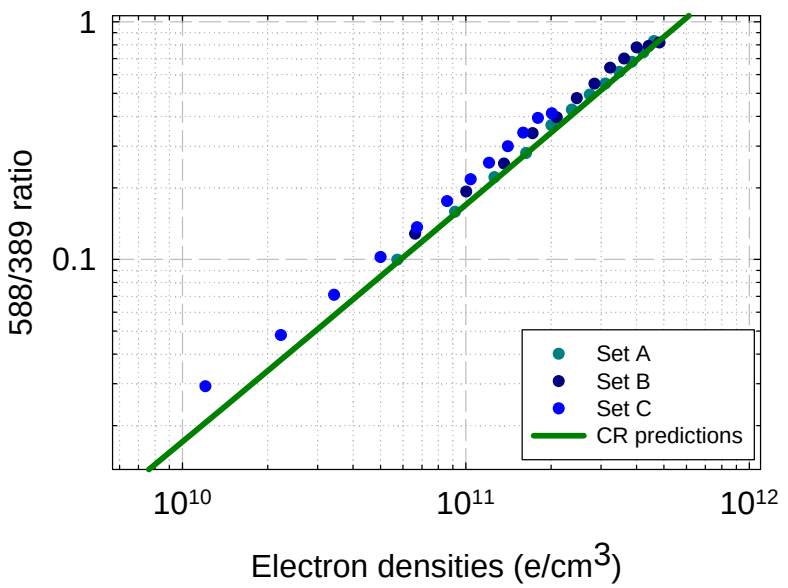

Density measurements obtained at different times essentially overlay each other

[447]/[588] ratio captures trends but misses absolutes

- **Anticipated T_e trends are observed**
  - High temperature at start, low temperatures later on
- **Measure T_e trends mimic computed trends**
  - Discrepancy in absolute values are apparent

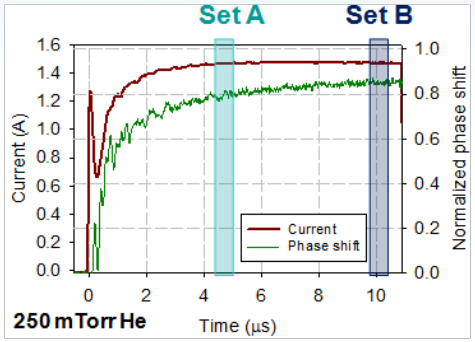

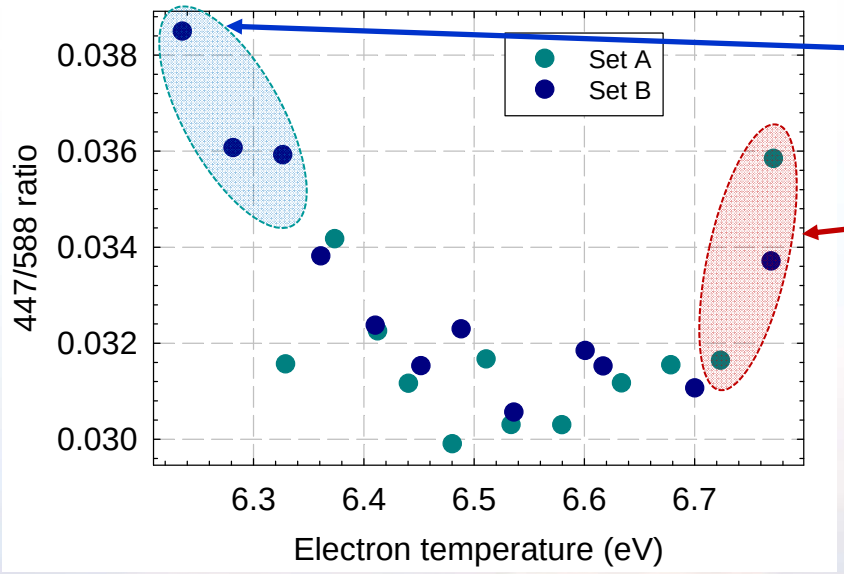

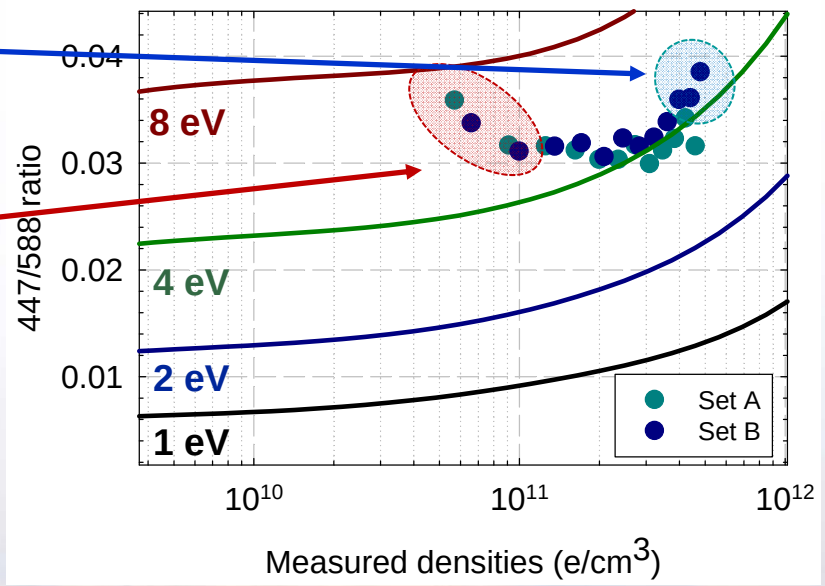

Uncertainties in rates, EEDF and/or interpolation of T_e from drift parameters should impact absolute values

Part III: Applications of LCIF

- **Applications of LCIF**
  - ion sheaths, double layers and positive columns

Ion sheath

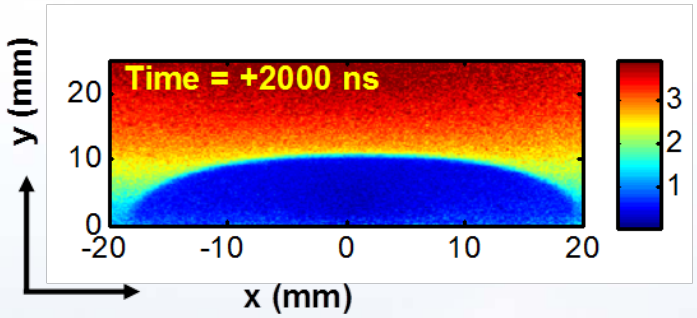

Double layers

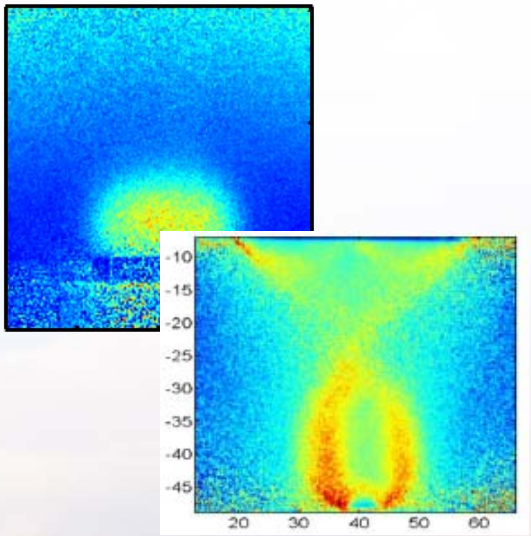

Striated positive column

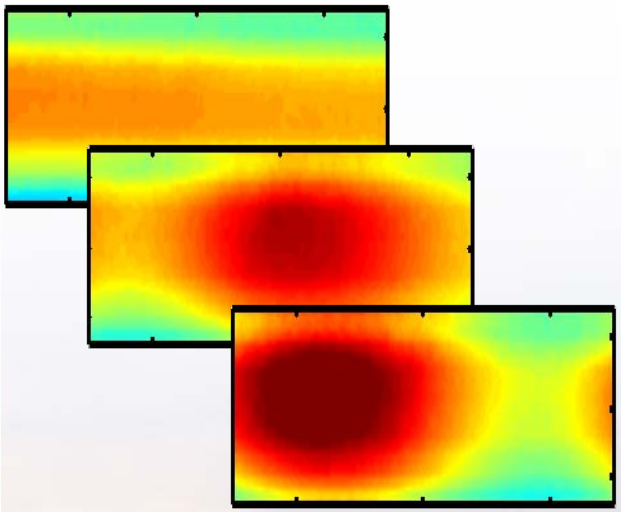

Emphasize structure and evolution of the plasma being studied

Demonstration of LCIF technique: 2D-sheath formation

- **Examine evolution and structure of ion sheath**
  - - 1 kV bias applied to inner electrode, 50 μs into afterglow (low n_e, low kT_e)
  - 20 ns snapshots of LCIF, 30 ns steps

Setup

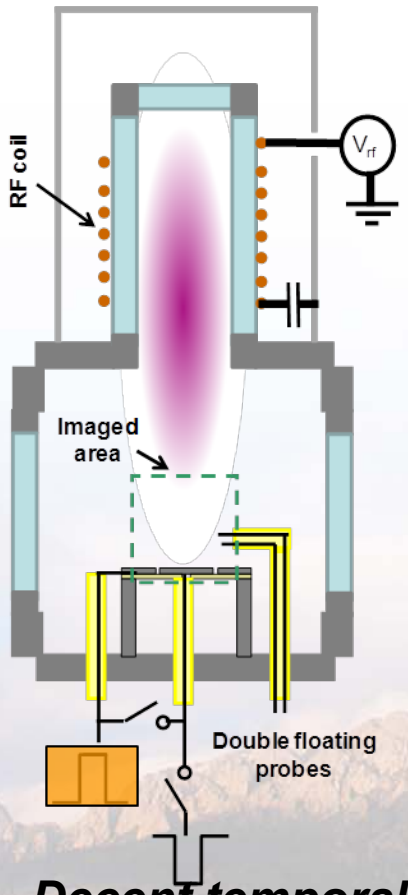

Data

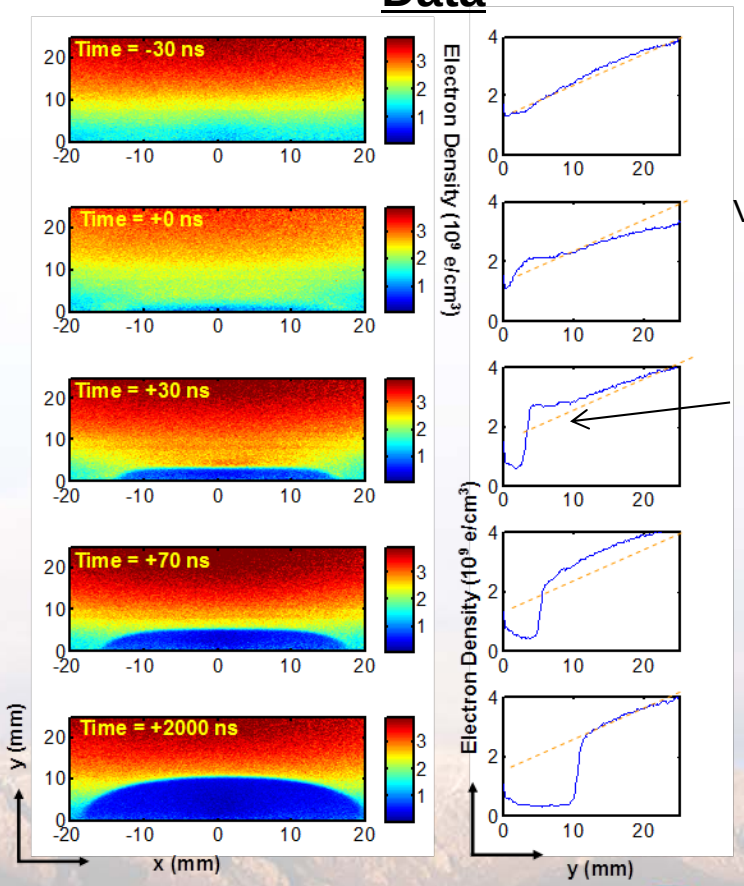

Initial structure

Voltage applied

"Matrix" sheath

Sheath evolving

Final sheath structure

Decent temporal and spatial resolution demonstrated

Interesting structure observed in the sheath

- **LCIF signal observed deep in the sheath**
  - Some caused by neutrals, but not all

2D Images

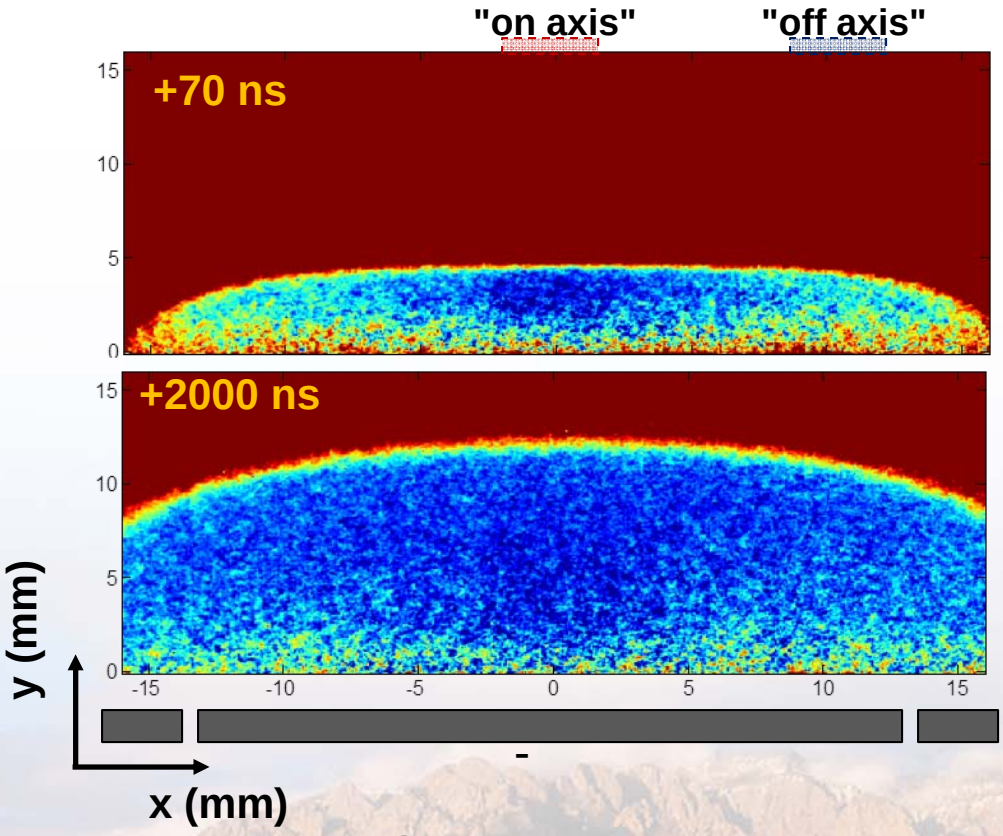

Profiles

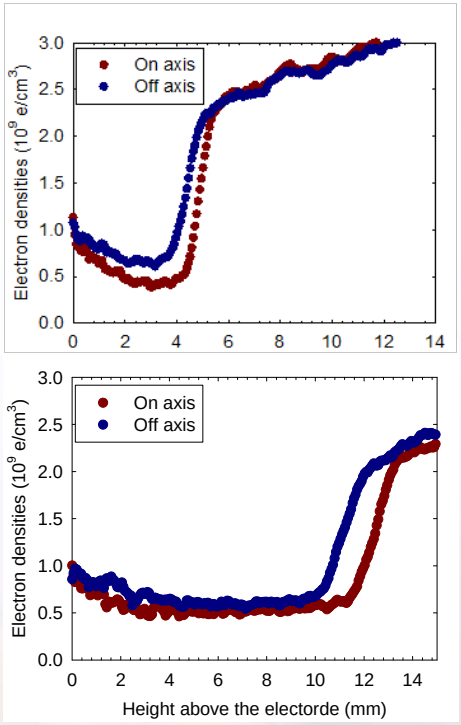

Signal deep in the sheath caused by electrons emitted from the electrode

Electrons backfill ion sheath after voltage is removed

- **LCIF detects electrons but not ions**
  - Examine time immediately after voltage is removed

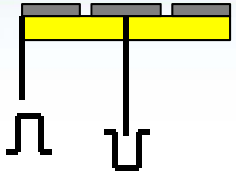

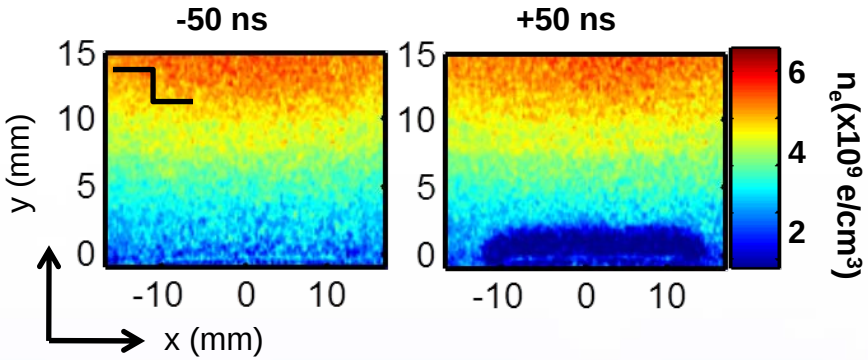

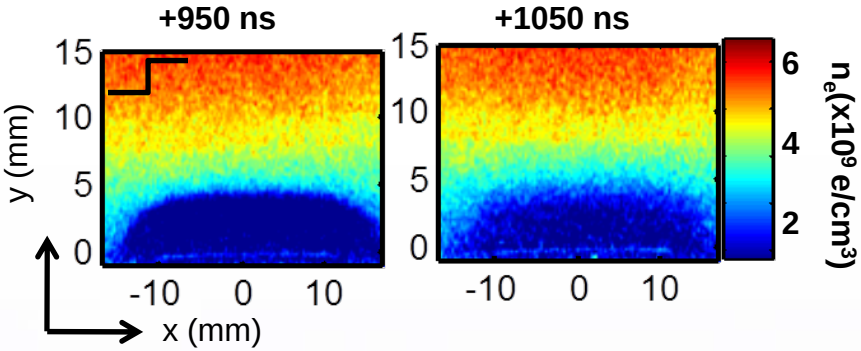

Negative Pulse

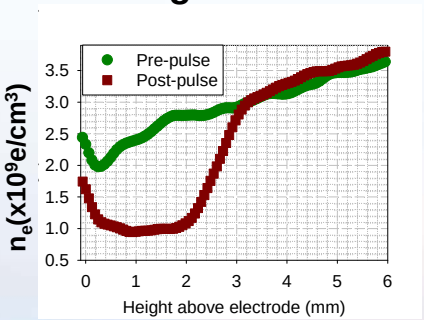

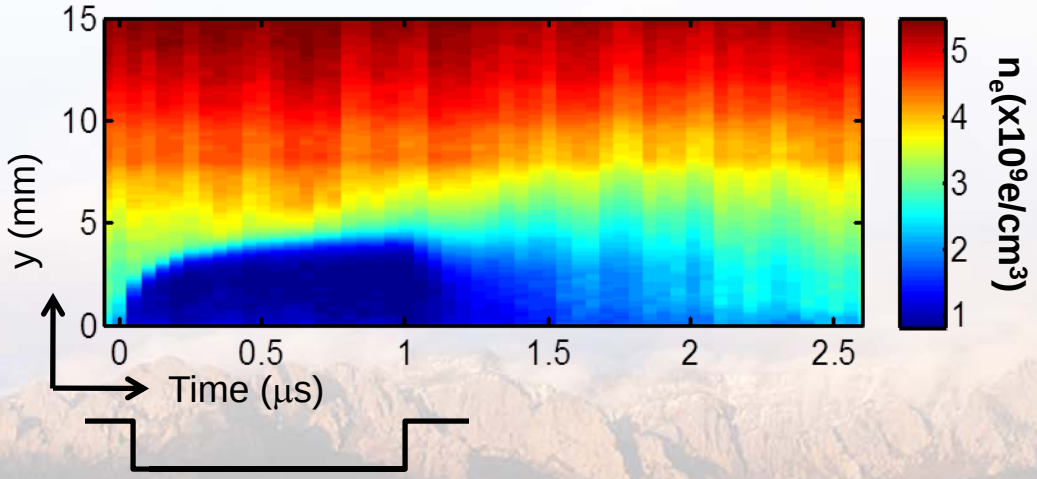

Positive Pulse

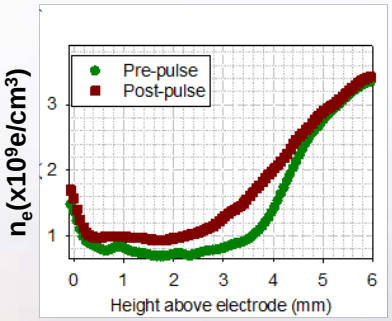

Ion densities can be quantified after voltage is removed

Sandia National Laboratories

Transient anodic double layer observed after pulsed excitation

- **Closer analysis of initial plasma distribution**
  - Use smaller (25 mm) diameter electrode, 100 mTorr afterglow

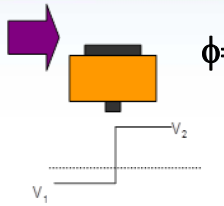

Earlier times

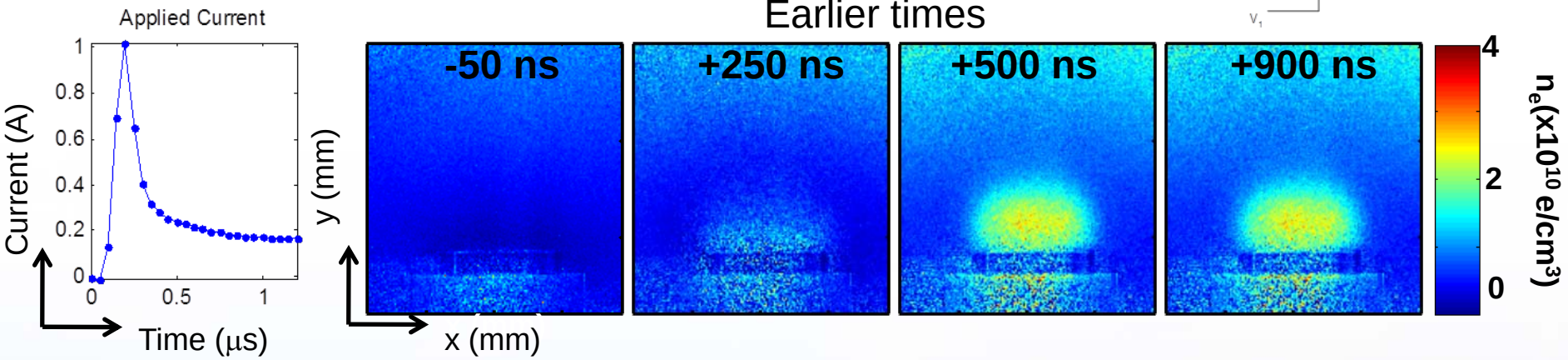

Later times

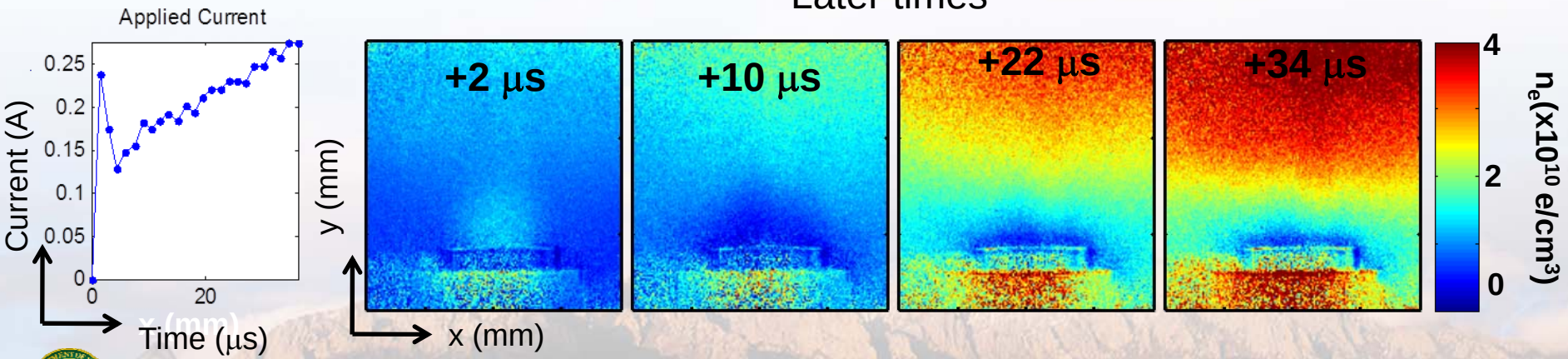

Structure undergoes inversion after stagnation

Higher energy electrons observed around edge of anode plasma

- **Temperature measurements made for +900 ns case**
  - Challenging measurement because of low level signals

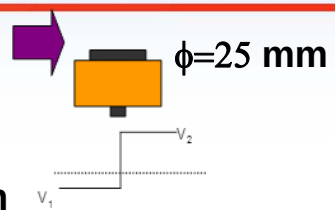

LCIF Data

388 nm

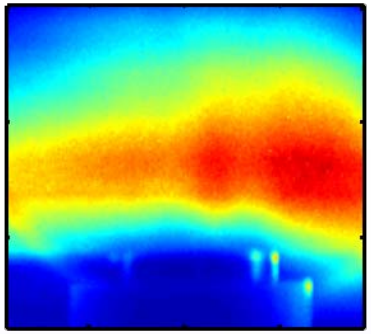

589 nm

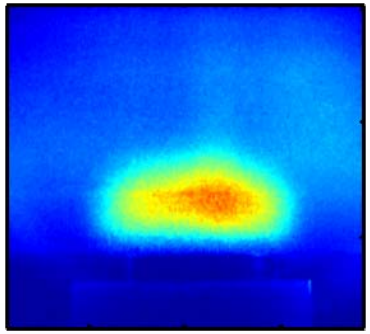

447 nm

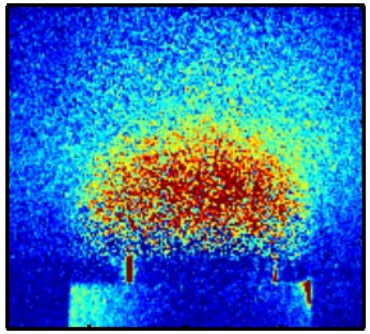

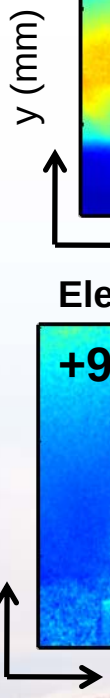

Analysis

Electron Densities

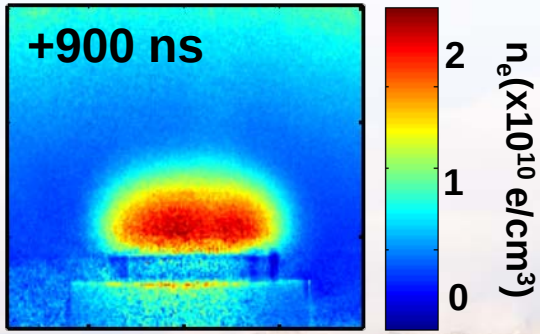

Electron Temperatures

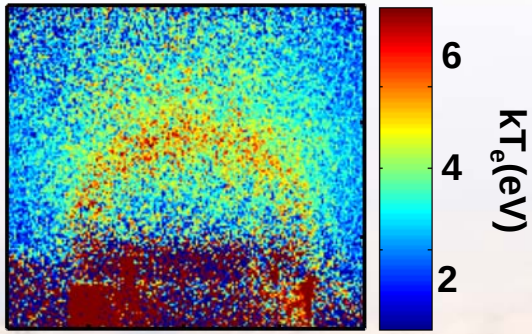

"Anodic Fireball"

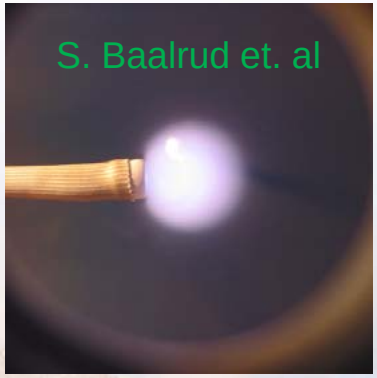

Electrons energized by localized electric fields supporting double layer

S. D. Baalrud , B. Longmier and N Hershkowitz, Plasma sourc. Sci. Technol. 18 035002 (2009)

Double layer more pronounced in ECR based plasma cathodes

- **NASA driven research interested in electron sources for propulsion**
  - Understand limitations on current extraction
- **Host Brandon Weatherford (U. Mich.) to implement LCIF**
  - Examine coupling of between plasma generation and electron extraction

Setup

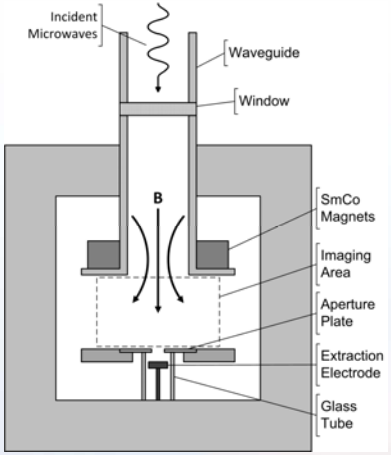

"Full color" picture

Density

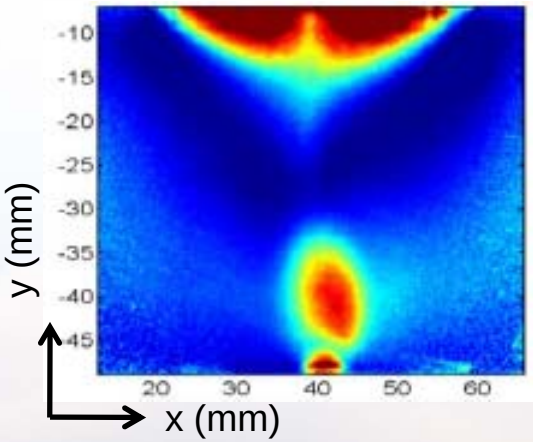

Temperature

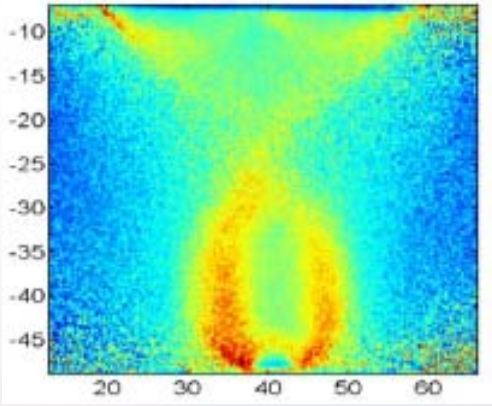

Multi-structure plasma formed by electron-extracting electrode...
… quite difficult to probe with more conventional means!

Sandia National Laboratories

LCIF is being used to study structure in a positive column

- **Positive column is "well understood" system**
  - Studied extensively, use it for calibration
- **Platform for fast ionization wave (FIW) studies**
  - Observations may warrant their own study

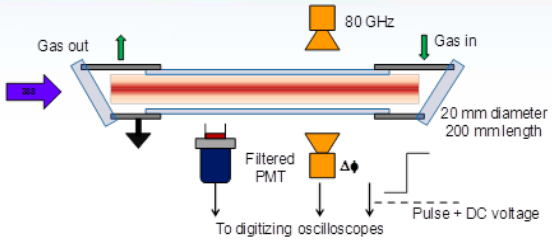

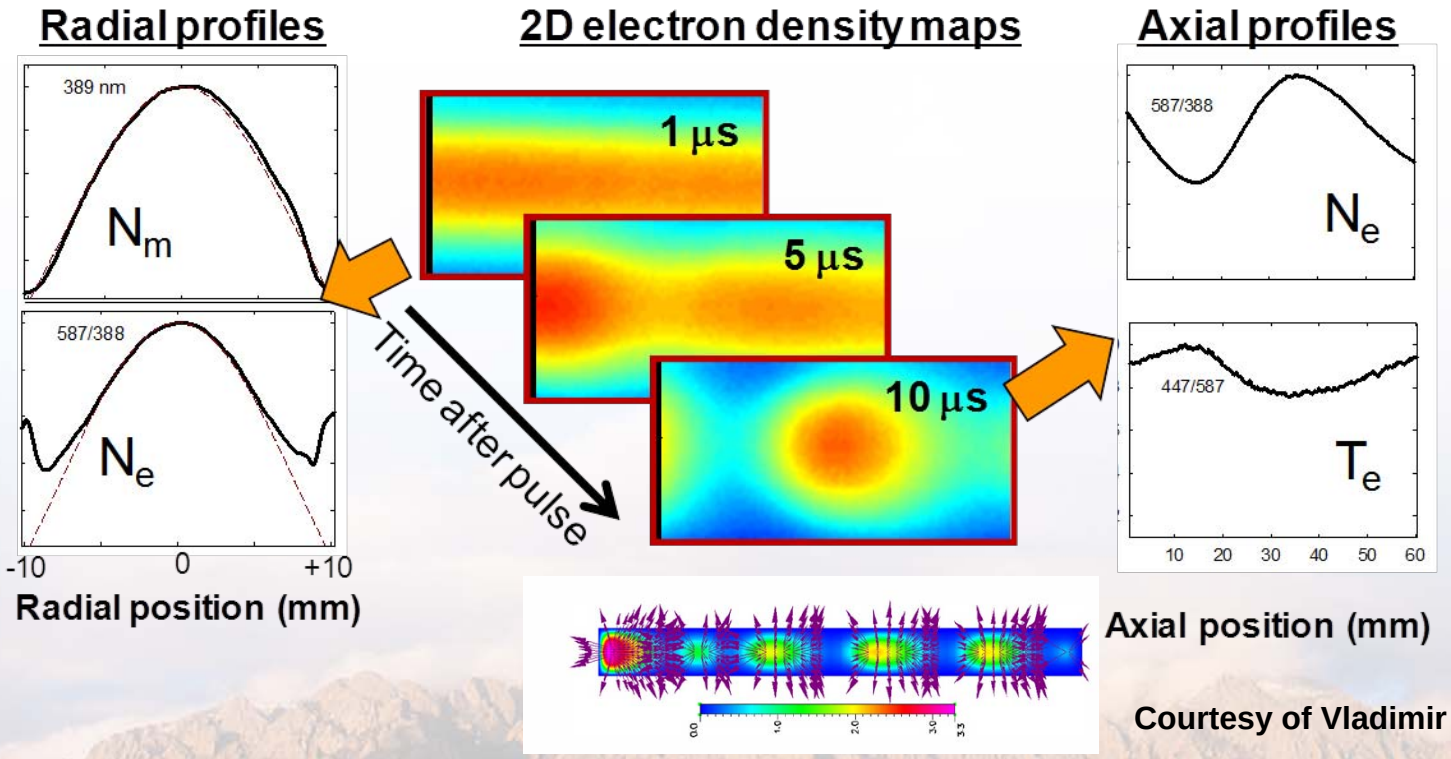

Courtesy of Vladimir Kolobov

Benchmark 2D simulations with measurements made by LCIF

V. Kolobov, J. Phys. D: Appl. Phys. **39** (2006) R487

Part IV: Future pursuits with LCIF

- **Extension of LCIF technique to other operating regimes**
  - Limitations of helium and paths around this….

Extension of helium

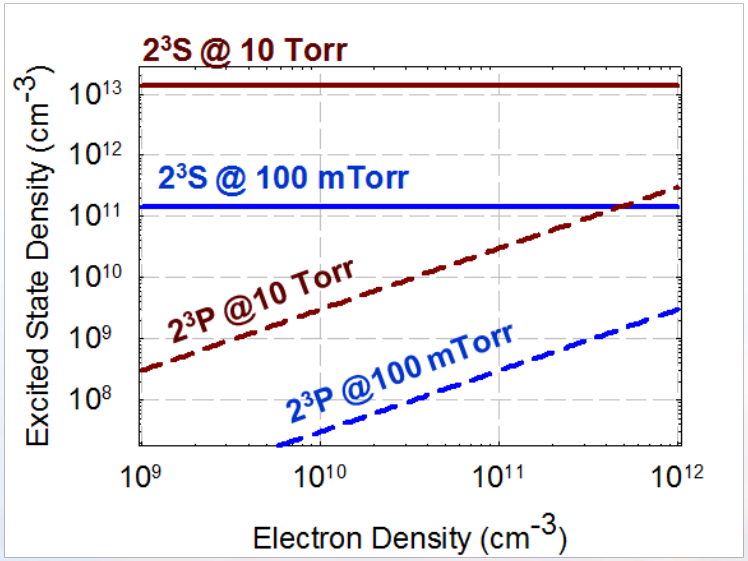

Argon LCIF

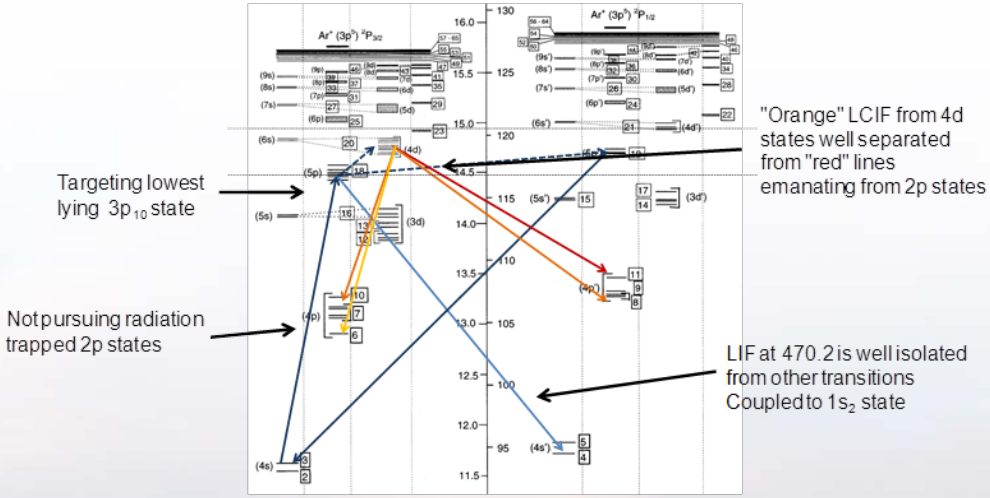

Helium becomes limited at higher pressures

- **Helium proved to be well suited for lower pressure and lower densities**
  - Limited spectroscopic pathways
  - Well known cross-sections
  - Highly populated, long lived 2^3S metastable state

- **As density increases and as composition changes**
  - Radiation trapping/transport becomes problematic

$$\tau = L / l_{mfp} \approx f_{nm} \lambda \left(Mc^2 / kT_A \right)^{1/2} N_A L << 1$$

Transition	f_{nm}	τ
$3^3P \rightarrow 2^3S$	0.064	>1
$4^3P \rightarrow 2^3S$	0.02	~1

(Assuming L=1 cm and $N_A \sim 10^{13}$ absorbers/cm^3)

States connected to 2^3S can become trapped do to strong coupling and higher populations

Pump out of alternative helium states

- **At higher pressures and densities, 2^3P state becomes adequately populated**
  - Comparable oscillator strengths (into comparable levels)
  - Sufficiently lower population compared to 2^3S

Scaling

2^3S State:

$$n_{2(3)S} \sim \frac{K^e_{0->S}}{K^e_{S->P}} n_0 \sim 10^{-5} n_0$$

2^3P State:

$$n_{2(3)P} \sim \frac{1}{A_{P->S}} \left[K^e_{0->P} + K^e_{S->P} \right] n_0 n_e$$

Trends

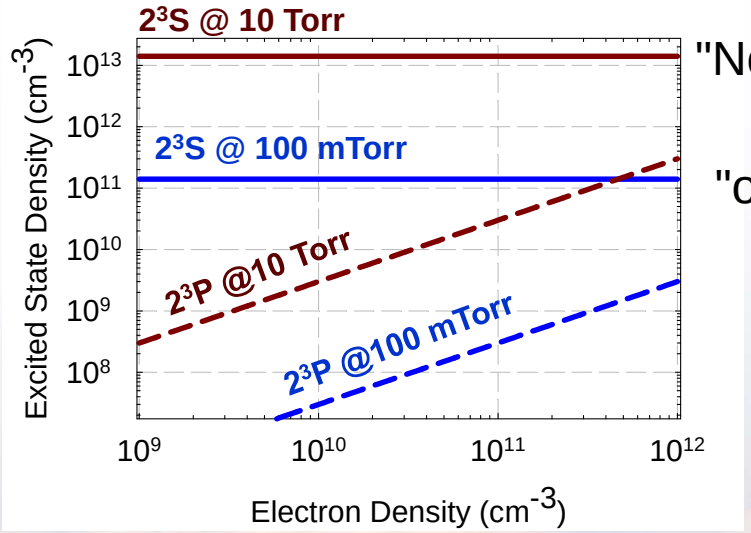

"Not ok"

"ok"

Low 2^3P state densities should be high enough to pump but low enough not to trap

Spectroscopic pathway proposed for pumping from 2^3P

- **Lower base density of 2^3P advantageous, but some tradeoffs**
  - Lose the nice "temperature free" 3^3P -> 3^3D transition
  - Spectrally dense - many transitions ~ 400 nm

Previous approach

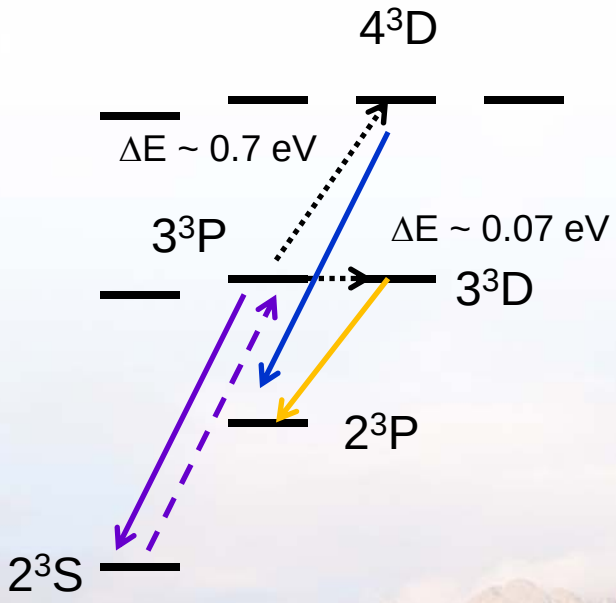

Proposed approach

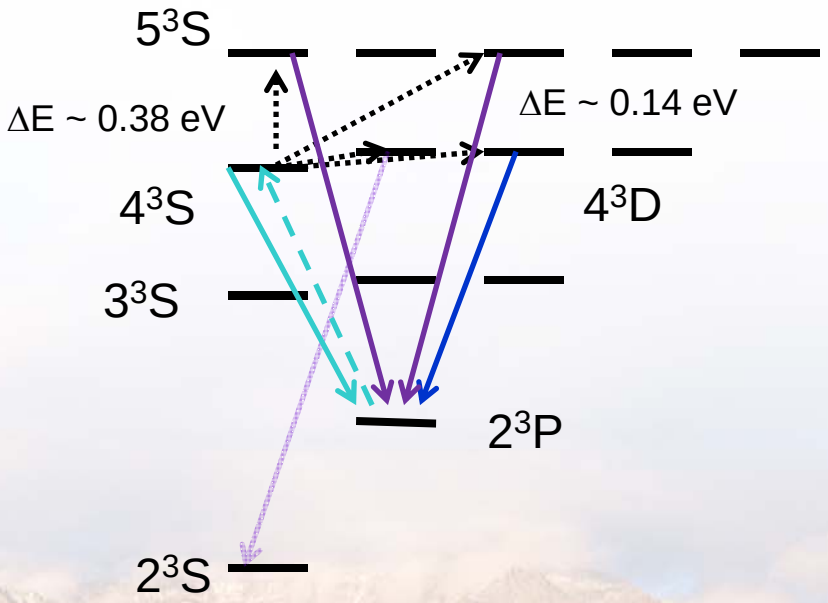

Pumping to the 3^3S or the 3^3D states are not "off the table" and may be perused

Preliminary investigation of proposed scheme looks promising

- **Employ same pulsed positive column used for 2^3S excitation**
  - Limit observations to states coupled to 2^3P
  - Integration of 20 ns, 10 ns after laser excitation

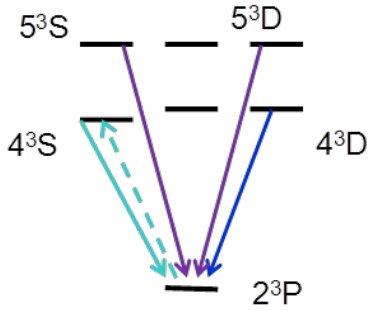

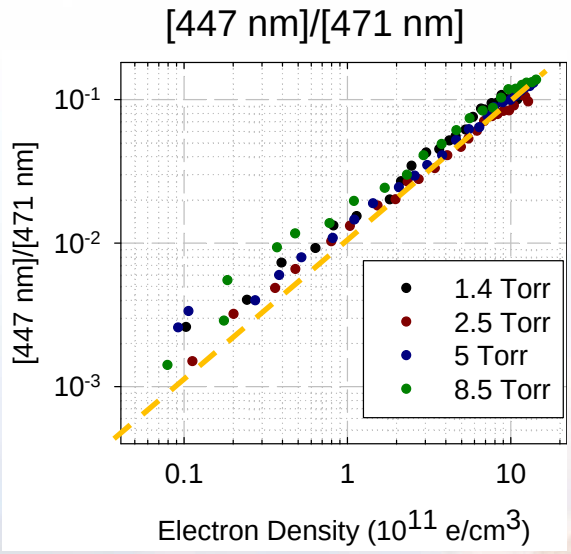

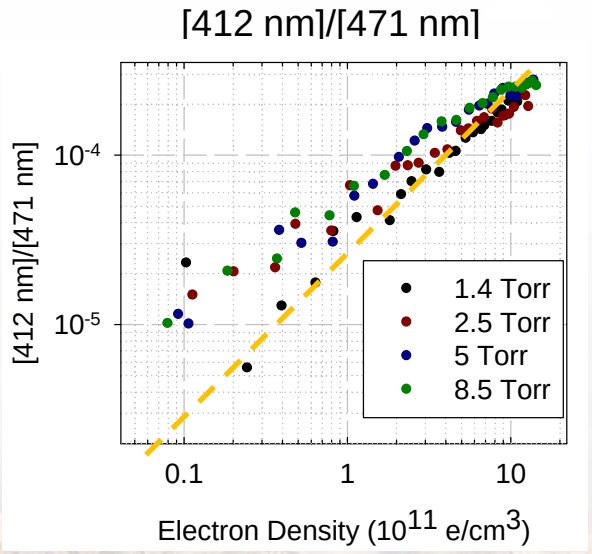

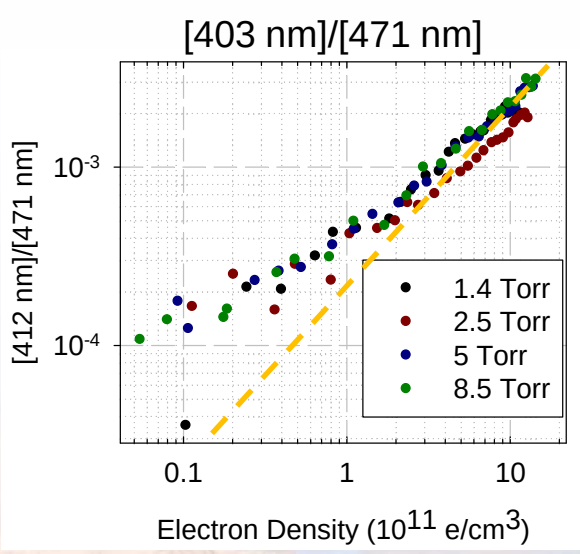

Alternative gasses are being considered

- **Technique is extendable to other gases**
  - Helium is seldom "gas of choice"
  - Helium becomes problematic in mixtures
- **Argon is commonly used gas and obvious choice**
  - More pump-probe pathways to consider
  - Individual lower lying $1s_x$ states are anticipated to less populated

$$\tau = L / l_{mfp} \approx f_{nm} \lambda \left(Mc^2 / kT_A \right)^{1/2} N_A L << 1$$

Helium

Transition	f_{nm}	τ
$3^3P \rightarrow 2^3S$	0.064	>1
$4^3P \rightarrow 2^3S$	0.02	~1

Argon

Transition	f_{nm}	τ
$2p_{10} \rightarrow 1s_5$	0.17	>>1
$3p_{10} \rightarrow 1s_5$	9×10^{-4}	0.08

(Assuming L=1 cm and $N_A \sim 10^{13}$ absorbers/cm^3)

Low oscillator strengths and possibly lower densities make argon attractive

Sandia National Laboratories

Complexity of argon makes extension of LCIF "challenging"

- **Argon offers more spectroscopic pathways to pursue**

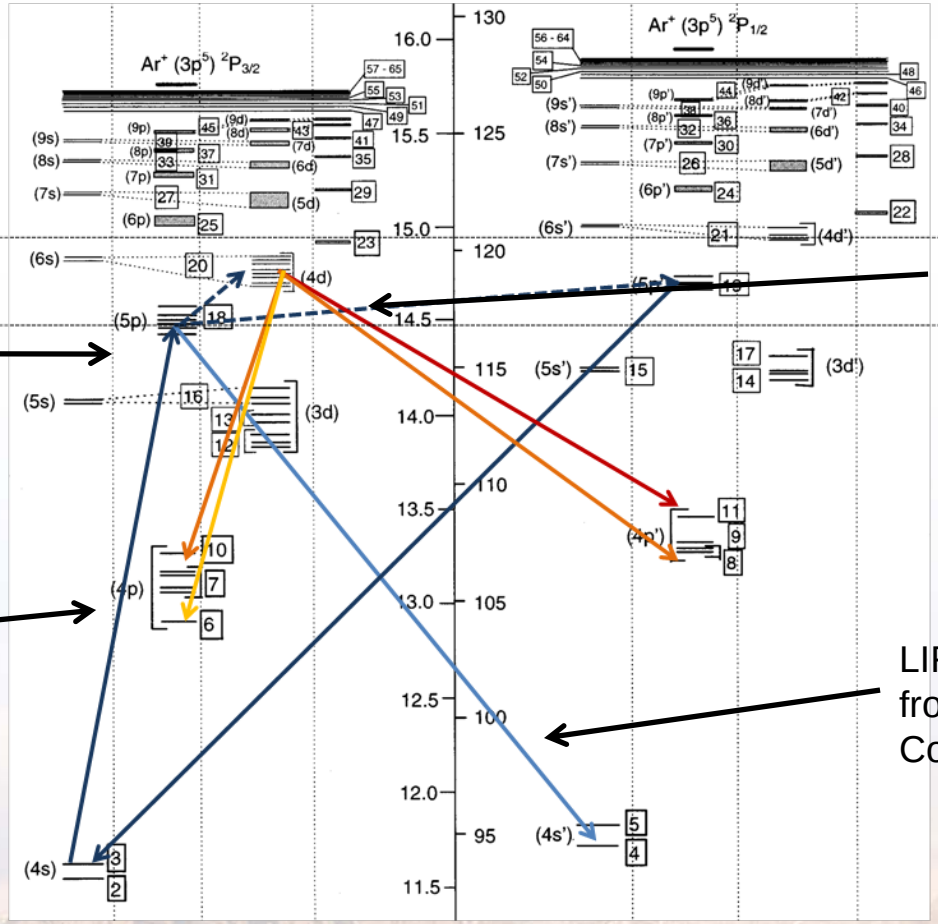

Targeting lowest lying $3p_{10}$ state

Not pursuing radiation trapped 2p states

"Orange" LCIF from 4d states well separated from "red" lines emanating from 2p states

LIF at 470.2 is well isolated from other transitions Coupled to $1s_2$ state

Taken from Bogearts et. al, J. Appl. Phys. **84**, 121, 1998

Cross sections and rates not well known for electronic driven processes from 3p to higher states

Despite reservations Argon LCIF is being investigated

- **Well characterized positive columnn is used to test feasibility**
  - Microwave interferometer to measure densities
  - Pulsed for higher densities/temperatures and stable plasmas
  - Time resolved LIF/LCIF with PMT + narrowband filters

Calibration cell

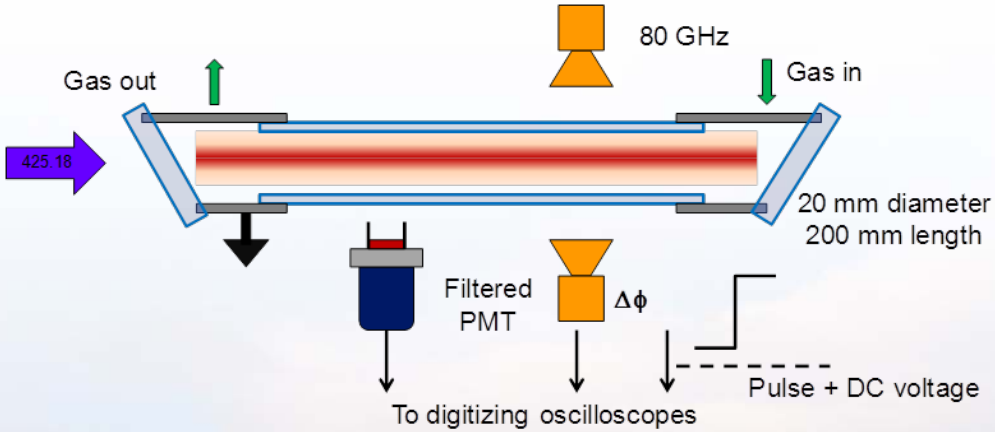

Preliminary trends

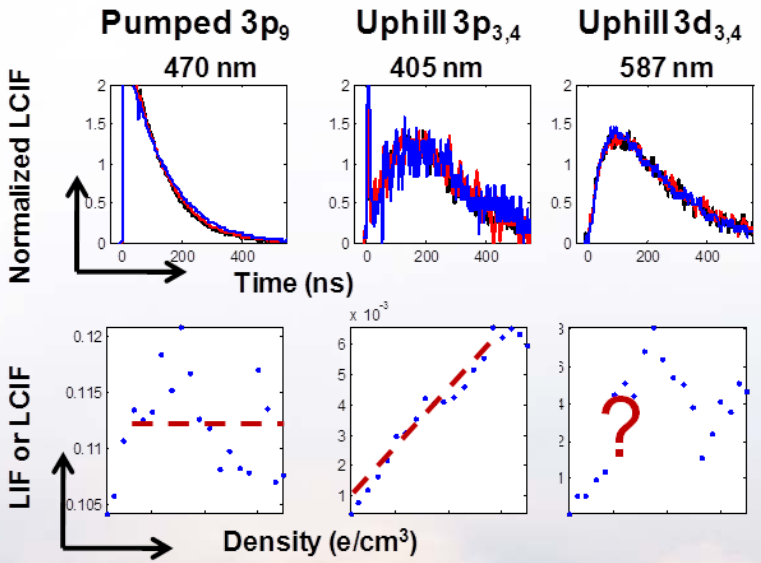

Perspective transitions are identified and calibration of the technique is underway …. Stay tuned!

Concluding remarks and future directions

- **LCIF technique demonstrated in 2D**
  - Free of “line of sight” constraints
  - Good spatial resolution – limited by optical collection
  - Decent temporal resolution – limited by ICCD gate times & tolerable signals

- **Caution required for proper implementation of the technique**
  - Uncertainties about rates – Absolute bounds on measurements
  - Proper choice of model – Capture the required physics

- **Technique should be extendable over broad parameter space**
  - Higher pressures – neutral collisions
  - Smaller dimensions – scattering and access
  - Other atomic systems

This work was supported by the Department of Energy Office of Fusion Energy Science
Contract DE-SC0001939

Thank you

Neutral mixing of 3^3P and 3^3D needs to be considered

- **Proximity (energetically) of states means neutrals can transfer excited population to 3^3D**
  - Energy spacing between states is 0.067 eV ~ 780 K

Amount of 3^3D produced from 3^3P

$$\Delta N_{Electrons} \sim K^{e}_{P->D} n_e \Delta N_P \Delta t \quad \text{and} \quad \Delta N_{Neutrals} \sim K^{N}_{P->D} n_0 \Delta N_P \Delta t$$

Bound determined by setting the two equal

$$\frac{\Delta N_{Electrons}}{\Delta N_{Neutrals}} \sim \frac{K^{e}_{P->D} n_e}{K^{N}_{P->D} n_0} \sim 1$$

Solve for n_e

$$n_e \sim \frac{K^{N}_{P->D}}{K^{e}_{P->D}} n_0 \sim \frac{10^{-12}}{10^{-5}} n_0$$

Pressure dependent density bound

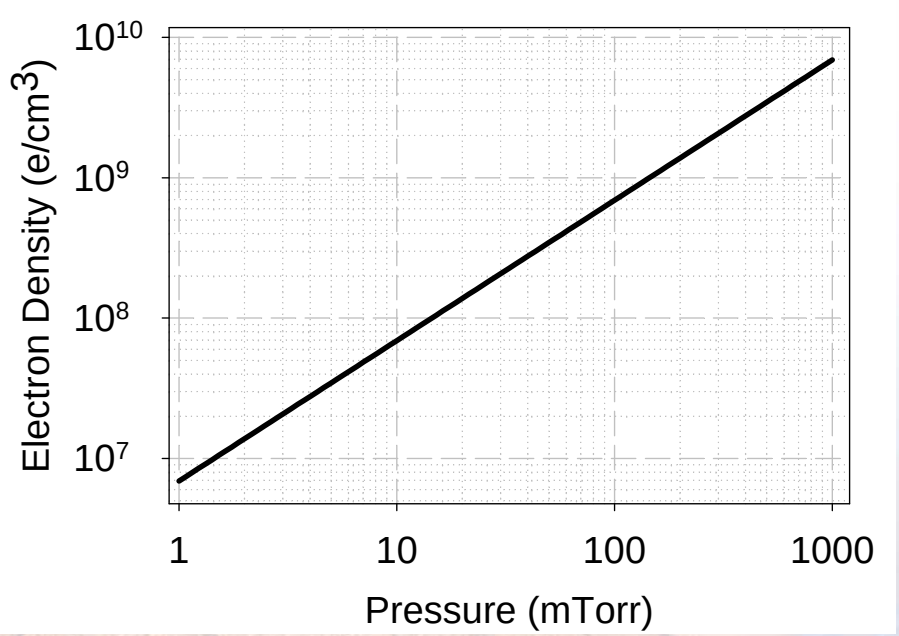

Lower limit on electron density scales with pressure (and temperature) of neutral background

R. Denkelmann, S. Freund and S. Maurmann, Contrib. Plasma Phys. **40**, 91 (2000).

References for rates and cross-sections

- **Superelastic**
  - Klein Rosseland
  - Sobelman

$$K_{ij}^{e} = \left\langle \sigma_{ij} v_e \right\rangle = \left(\frac{m_e}{2\pi k T_e} \right)^{3/2} \int_0^{\infty} \sigma_{ij}(v) \exp\left(\frac{-m_e v^2}{2 k_B T_e} \right) 4\pi v^2 dv \left[\frac{g_j}{g_i} \exp\left(\frac{\left(E_j - E_i\right)}{k_B T_e} \right) \right]$$

[1] C. F. Burrell and H.-J. Kunze, Phys. Rev. A **18**, 2081 (1978).
[1] P. Chall, E. K. Souw and J. Uhlenbusch. J. Quant. Spectrosc. Radiant. Transfer **34**, 309 (1985).
[1] G. Dilecce, P. F. Ambrico and S. De Benedictis, J. Phys. B: At. Mol. Opt. Phys. **28**, 209 (1994).
[1] R. Denkelmann, S.Maurmann, T. Lokajczyk, P. Drepper, and H. –J. Kunze, J. Phys. B: At. Mol. Opt. Phys. **32**, 4635 (1999).
[1] R. Denkelmann, S. Freund and S. Maurmann, Contrib. Plasma Phys. **40**, 91 (2000).
[1] K. Tsuchida, S. Miyake, K. Kadota and J. Fujita, Plasma Physics **25**, 991 (1983).
[1] B. Dubreuil and P. Prigent, J. Phys. B: At. Mol. Opt. Phys. **18**, 4597 (1985).
[1] E. A. Den Hartog, T. R. O'Brian and J. E. Lawler, Phys. Rev. Lett. **62**, 1500 (1989).
[1] K. Dzierzega, K. Musiol, E. C. Benck and J. R. Roberts, J. Appl. Phys. **80**, 3196 (1996).
[1] L. Maleki, B. J. Blasenheim, and G. R. Janik, J. Appl. Phys. **68**, 2661 (1990).
[1] R. S. Stewart, D. J. Smith, I. S. Borthwick and A. M. Paterson, Phys. Rev. E **62**, 2678 (2000).
[1] R. S. Stewart, D. J. Smith, J. Phys. D: Appl. Phys. **35**, 1777 (2002).
[1] A. Hidalgo, F. L Tabares and D. Tafalla, Plasma Phys. Control. Fusion **48**, 527 (2006).
[1] D. A. Shcheglov, S. I. Vetrov, I. V. Moskalenko, A. A. Skovoroda and D. A. Shuvaev, Plasma Phys. Rep. **32**, 119 (2006).
[1] M. Krychowiak, Ph Mertens, R. Konig, B. Schweer, S. Brezinsek, O. Schmitz, M. Brix, U. Samm and T. Klinger, Plasma Phys. Control. Fusion **50**, 65015 (2008).
[1] K. Takiyama, H. Sakai, M. Yamasaki, and T. Oda, Jpn. J. Appl. Phys. **33**, 5038 (1994).
[1] M. Watanabe, K. Takiyama, H. Toyota Jpn. J. Appl. Phys. **38**. 4380 (1999).
[1] G. Nersisyan, T. Morrow, and W. G. Graham, Appl. Phys. Lett. **85**, 1487 (2004)
[1] W. L Wiese, M. W. Smith, and B. M. Glennon, *Atomic Transition Probabilities* ***4/V1*** (Nat. Stand. Ref. Data. Ser., Nat. Bur. Stand. Washington DC, 1966).
[1] Yu. Ralchenko, R. K. Janev, T. Kato, D. V. Fursa, I. Bray, F. J. De Heer, Atomic Data and Nuclear Data Tables **94**, 603 (2008).
[1] I.I. Sobelman, L. A. Vainshtein, and E. A. Yukov, *Excitation of Atoms and Broadening of Spectral Lines* (Springer, New York, 1981) p. 5.

$$K_{ij}^{e} = \left\langle \sigma_{ij} v_e \right\rangle = \left(\frac{m_e}{2\pi k T_e} \right)^{3/2} \int_0^{\infty} \sigma_{ij}(v) \exp\left(\frac{-m_e v^2}{2 k_B T_e} \right) 4\pi v^3 dv$$

Further experiments point to where improvement is needed

- **Here is the "ugly" data**
  - Predicted trends approach measured trends
- **Two data sets offer some clues**
  - Low pump power and low concentration of species
- **Stimulated emission inducing 3^3P to 3^3S transition?**
  - Population inversion: $N_P >> N_S$ after excitation

Spontaneous Emission ***Stimulated emission & absorption***

$$\frac{dN_S}{dt} = AN_P + A\left(\frac{\lambda^2}{8\pi}\right)g(\nu)\left(N_P - \frac{g_2}{g_1}N_S\right)\frac{I}{h\upsilon}$$

After pumping inversion occurs

$$\frac{dN_S}{dt} \approx A_{eff}N_P, \quad N_P >> N_S$$

Where

$$A_{Eff} = A\left[1+\left(\frac{\lambda^2}{8\pi}\right)g(\nu)\frac{I}{h\upsilon}\right] > 10^8 s^{-1}?$$

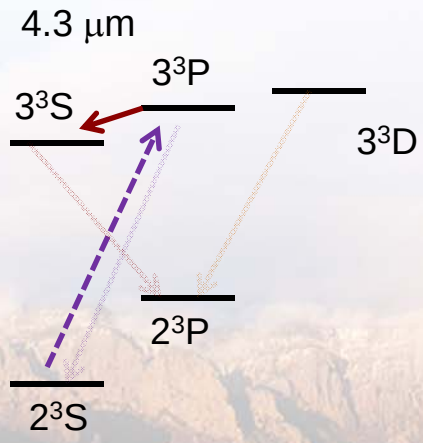

Photon density ***Gas density***

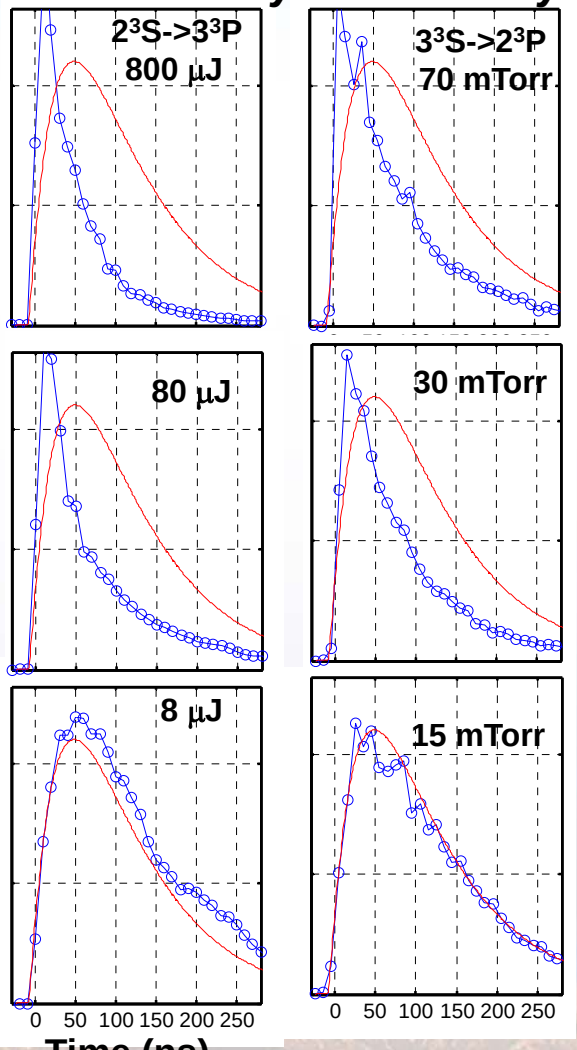

More complete treatment should include photon densities

Complete treatment bypassed through simplifying approximations

- **Assume population inversion occurs only during laser excitation**
  - Side step need to track absolute photon intensities

$$A_{Eff} = A_{Nom}\left[1 + A_{Inv}e^{-\frac{I_{Laser}}{I_{Threshold}}}\right]$$

Normalized time resolved trends

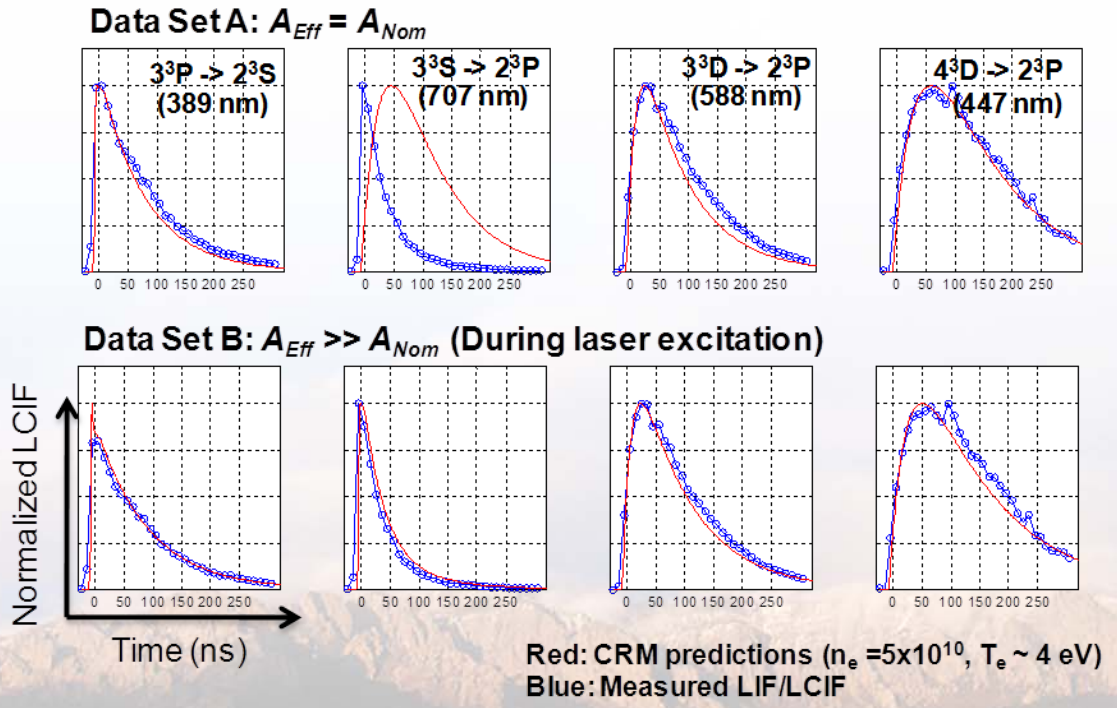

Simplifying assumption produces trends consistent with observation

Sandia National Laboratories

Key uphill transitions are not significantly impacted by radioactive coupling

- **Dominant population pathway is still through excited 3^3P state**
  - Final densities of 3^3P state will change, but this is normalized out in analysis

Averaged trends

Data Set A: $A_{Eff} = A_{Nom}$

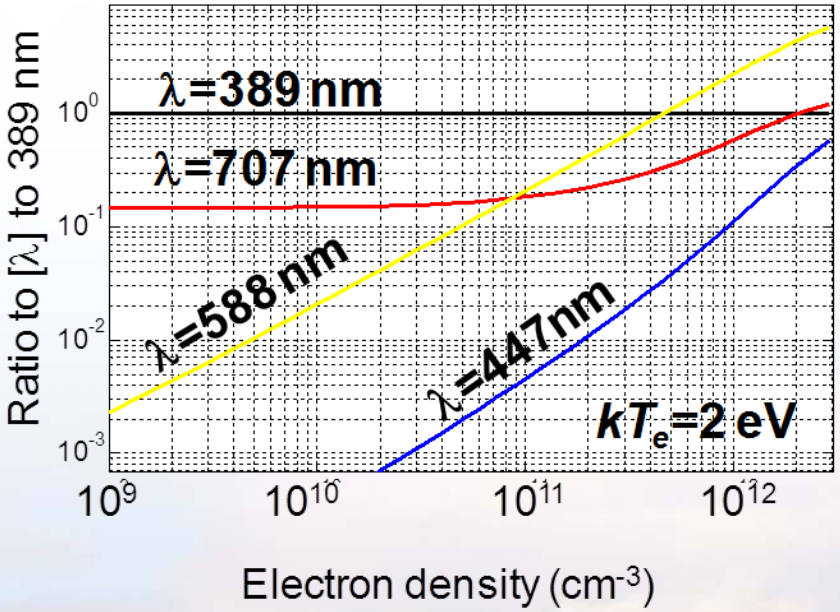

Data Set B: $A_{Eff} >> A_{Nom}$ (During laser excitation)

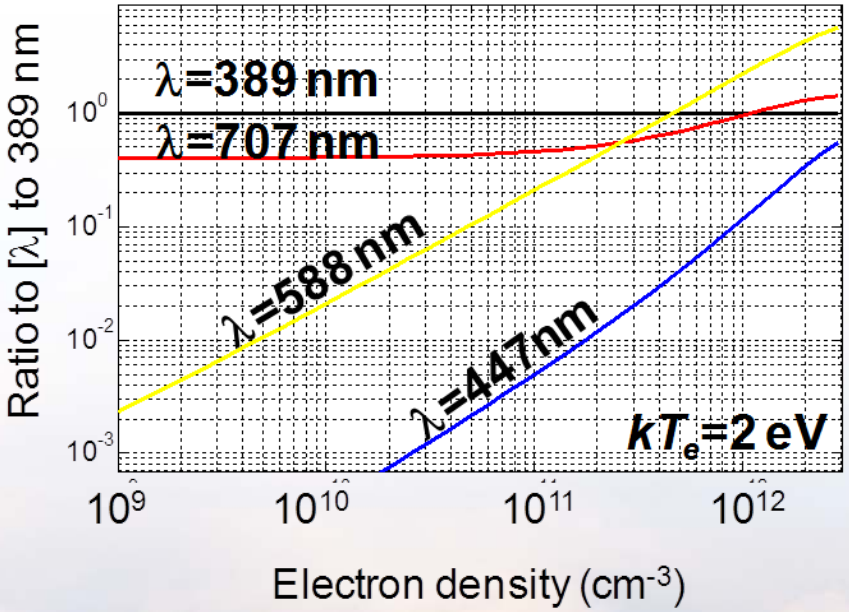

Caution should still be used if considering the 3^3S state for normalization

[447]/[588] ratio captures trends but misses absolutes

- **Anticipated T_e trends are observed**
  - High temperature at start, low temperatures later on
- **Measure T_e trends mimic computed trends**
  - Discrepancy in absolute values are apparent

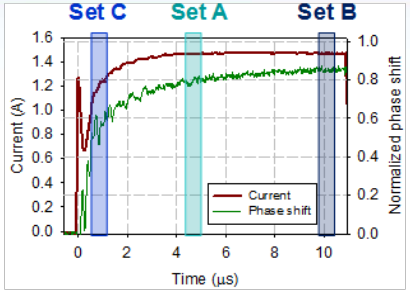

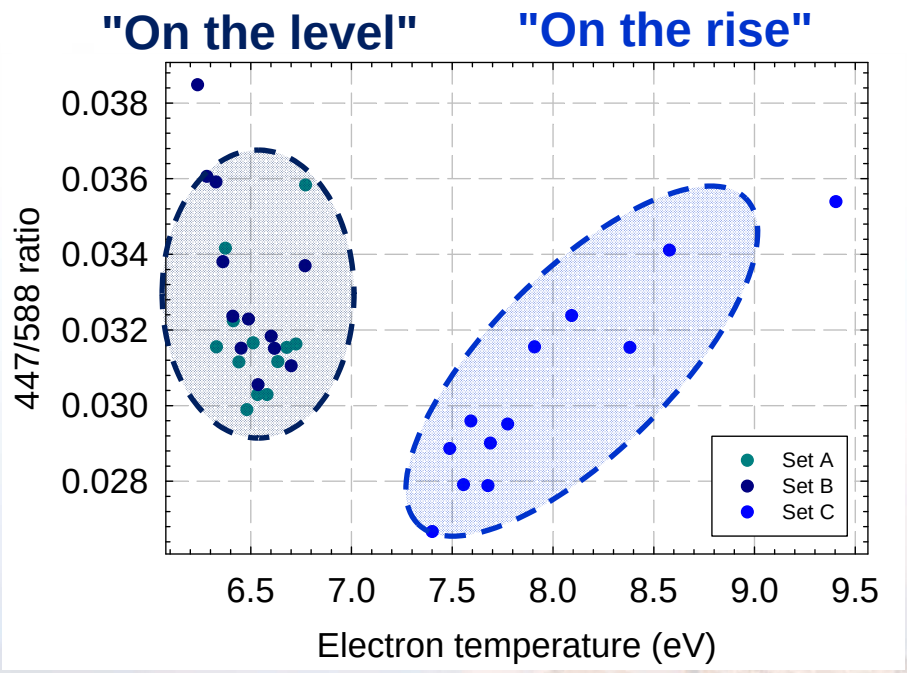

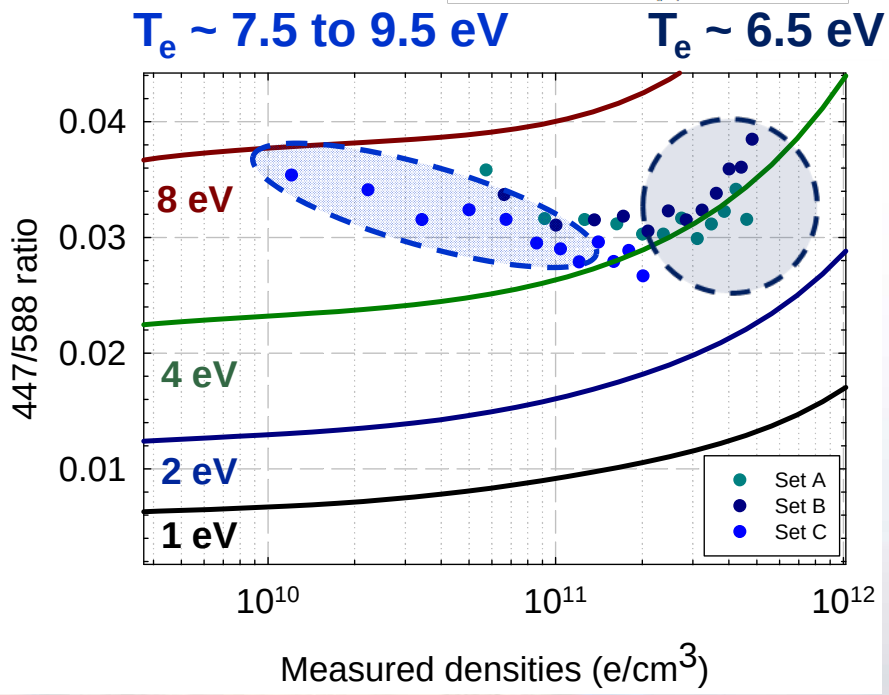

Uncertainties in rates, EEDF and/or interpolation of T_e from drift parameters should impact absolute values

Analysis of ion-matrix sheath is used to further test LCIF technique

- **Immediately after the pulse is applied**
  - Electrons are rapidly pushed away from electrode
  - But ions should have little time to respond

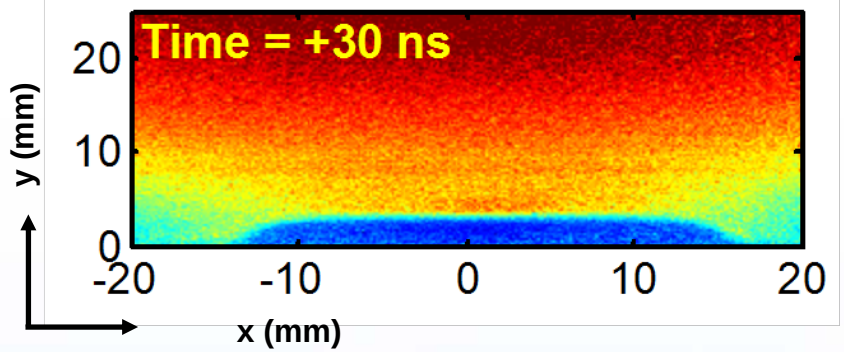

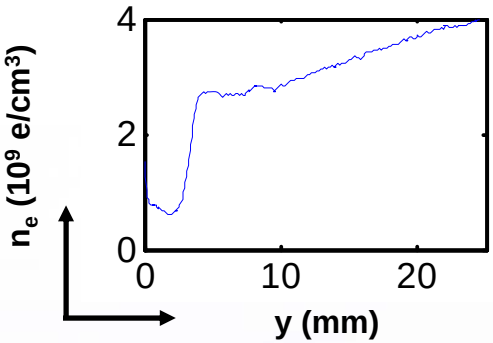

- **Using Poisson's equation and assuming quasi neutrality before the application of the pulse:**

$$\nabla^2 V = \frac{e}{\varepsilon_0} n \longrightarrow n_i \approx \frac{2\varepsilon_0 V}{e\Delta x^2}$$

- **For a voltage of 1 kV and a thickness of ~ 5 mm:**

$n_e \sim 4 \times 10^9$ electrons/cm^3

Reasonable cross-check of LCIF technique

Preliminary survey points to useful transitions

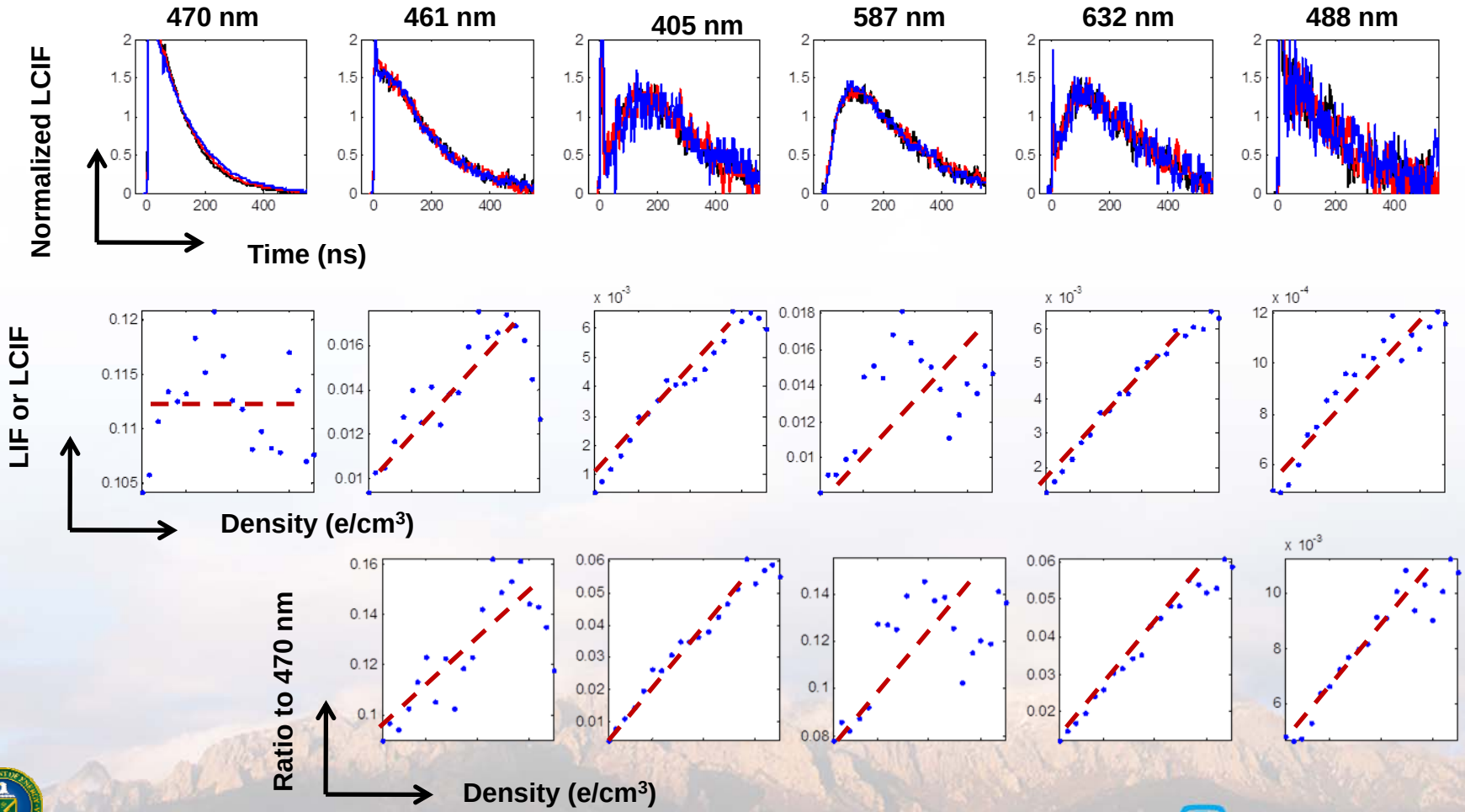

Preliminary investigation of proposed scheme looks promising

Extracted E/N

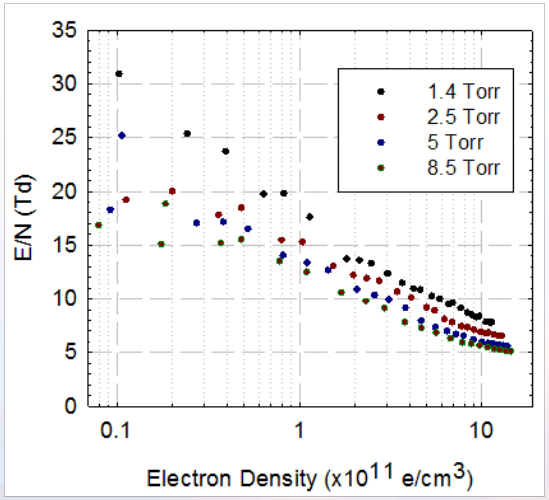

[412 nm]/[447 nm]

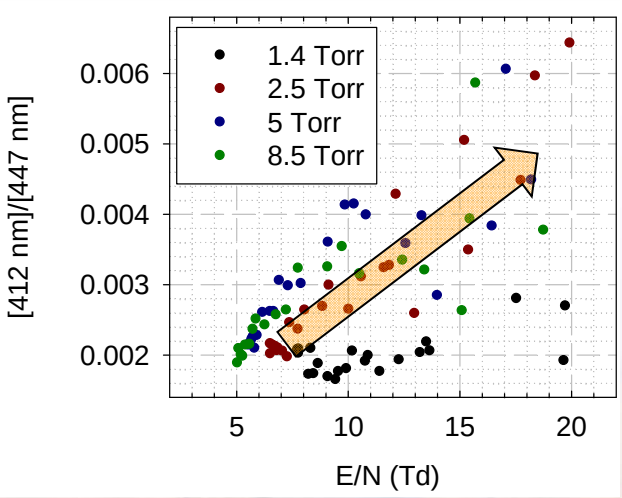

[403 nm]/[447 nm]